INORGANIC
CHEMISTRY
FRONTIERS

CrossMark
click for updates

Enhancing the photoluminescence quantum yields of blue-emitting cationic iridium(III) complexes bearing bisphosphine ligands†

Diego Rota Martir,[a] Ashu K. Bansal,[b] Vincent Di Mascio,[a] David B. Cordes,[a] Adam F. Henwood,[a] Alexandra M. Z. Slawin,[a] Paul C. J. Kamer,[a] Laura Martínez-Sarti,[c] Antonio Pertegás,[c] Henk J. Bolink,[c] Ifor D. W. Samuel[b] and Eli Zysman-Colman*[a]

Herein we present a structure–property relationship study of thirteen cationic iridium(III) complexes of the form of $[Ir(C^N)_2(P^P)]PF_6$ in both solution and the solid state through systematic evaluation of six bisphosphine (P^P) ligands (xantphos, dpephos, dppe, Dppe, nixantphos and isopropxantphos). All of the complexes are sky-blue emissive, but their photoluminescence quantum yields (Φ_{PL}) are generally low. However, strong and long-lived blue luminescence (λ_{em} = 471 nm; Φ_{PL} = 52%; τ_e = 13.5 μs) can be obtained by combining the reduced bite angle of the 1,2-bis-diphenylphosphinoethene (dppe) chelate with the bulky 2-(4,6-difluorophenyl)-4-mesitylpyridinato (dFmesppy) cyclometalating ligand. To the best of our knowledge this is the highest Φ_{PL} and the longest τ_e reported for cyclometalated iridium(III) complexes bearing bisphosphine ligands. Light-emitting electrochemical cells (LEECs) were fabricated using lead complexes from this study, however due in part to the irreversible electrochemistry, no functional LEEC was achieved. Organic light-emitting diodes were successfully fabricated but only attained maximum external quantum efficiencies of 0.25%.

Introduction

The expansion of low-cost and more efficient lighting sources based on phosphorescent materials is one of the greatest challenges of our century.[1] In particular, iridium complexes have attracted much attention due to their relatively short-lived triplet excited states (τ_e) and high photoluminescence quantum yields (Φ_{PL}), which are crucial properties for emitters employed in organic light emitting diodes (OLEDs) or light-emitting electrochemical cells (LEECs).[2] In addition, due to

the large variety of ligand families that are readily synthetically accessible, the emission color of iridium(III) complexes can be easily tuned across the entirety of the visible spectrum.[3] In the last decade, despite the reports of many phosphorescent green and red emitters[4] having been synthesised, the design of high-performance blue-emitting materials remains a challenge.[5] Recently, examples of sky-blue and deep-blue emitting cationic iridium complexes bearing biimidazole,[6] bis(NHC),[7] substituted triazole or tetrazole,[8] or pyrazolyl-pyridine[9] as ancillary ligands have been explored, but challenges still remain regarding efficiencies and stabilities of these emitters in devices.[10] Thus, there is still a demand for blue-emitting phosphors as emitters in lighting devices.

The vast majority of cationic iridium complexes possess the motif $[Ir(C^N)_2(N^N)]^+$, where C^N is a cyclometalating ligand with 2-phenylpyridinato (ppy) as the archetype and N^N is an ancillary ligand with 2,2′-bipyridine (bpy) as the archetype.[11] Despite their prominence as ligands in homogeneous catalysis,[12] phosphorus(III)-based ligands have remained underexplored in their complexation to iridium(III). Indeed, only a few examples have been reported implicating ligands with a P–Ir bond for optoelectronic applications; these include monodentate phosphines,[13] phosphinites, phosphonites,[14] phosphites,[15] bidendate benzyldiphenylphosphine P^C chelators,[16]

[a]Organic Semiconductor Centre, EaStCHEM School of Chemistry, University of St Andrews, St Andrews, Fife KY16 9ST, UK.
E-mail: eli.zysman-colman@st-andrews.ac.uk; http://www.zysman-colman.com;
Fax: +44 (0)1334 463808; Tel: +44 (0)1334 463826
[b]Organic Semiconductor Centre, SUPA, School of Physics and Astronomy, University of St. Andrews, St. Andrews, Fife KY16 9SS, UK. E-mail: idws@st-andrews.ac.uk
[c]Instituto de Ciencia Molecular, Universidad de Valencia, C/ Catedrático J. Beltrán, ES-46980 Paterna, Valencia, Spain. E-mail: henk.bolink@uv.es

other P^C ligands,[17] P^N[18] and P^P chelators.[19] Given the paucity of photoluminescent iridium complexes bearing phosphine ligands in general and P^P chelators in particular, we have sought to systematically explore the effect of differing the bisphosphine ancillary ligand on the properties of [Ir(C^N)$_2$(P^P)]PF$_6$ complexes. Bisphosphines potentially offer several advantages: (1) they confer chemical stability both in the solid state and in organic solvents due in part to their steric bulk;[16c,19a] (2) the electronic properties of the complexes remain highly tunable;[13a] (3) due to their strong σ-donating character, they inhibit d–d transitions through destabilization of the metal-centered (MC) antibonding orbitals, making radiative decay more favourable.[15,16d,19a] Improved organic light emitting diode (OLED) device performance has been achieved as a consequence of the use of phosphine-based ligands.[15,16c,17a]

We[2b,6a,8c,20] and others,[9,17c,19b,21] have been recently targeting the development of deep blue-emitting cationic iridium complexes, which are particularly relevant for light emitting electrochemical cells (LEECs), as an alternative solid-state lighting device architecture to OLEDs. In the context of [Ir(C^N)$_2$(P^P)]PF$_6$ complexes, Hor et al. recently reported the synthesis and the photophysical investigation of iridium(III) complexes bearing dppb (1,4-bis(diphenylphosphino)butane), dpephos (bis(2-diphenylphosphinophenyl) ether), nixantphos (2,4-bis(diphenylphosphino)phenoxazine) and xantphos (4,5-bis-diphenylphosphino-9,9-dimethylxanthene) P^P ancillary

ligands twinned with either ppy, 2-(4,6-difluorophenyl)pyridinato (dFppy) or 2′-phenyl-9-O-benzyl-10,11-dihydrocinchonine (pcn) C^N ligands.[19a] The bluest emission in their study (λ_{em}: 472 nm) was achieved with the complex [Ir(dFppy)$_2$(dppb)]PF$_6$, which exhibited a Φ_{PL} of 30% and bi-exponential emission decay kinetics (τ_e: 0.22, 0.02 μs) at room temperature in dichloromethane. Similar sky-blue emission (λ_{em}: 476 nm) was observed for the complex [Ir(dFppy)$_2$(xantphos)]PF$_6$, but in this case the Φ_{PL} was very low at 0.02 with very short bi-exponential lifetimes (τ_e: 0.004, 0.06 μs). Other instances of blue emission in MeCN solution within the same class of complexes include [Ir(ppy)$_2$(dppe)]$^+$ (λ_{em}: 459 nm, Φ_{PL}: 0.44%, τ_e: 0.29 μs),[19d] [Ir(ppy)$_2$(dppb)]$^+$ (λ_{em}: 459 nm, Φ_{PL}: 0.68%, τ_e: 0.52 μs),[19d] and [Ir(Fmppy)$_2$(dppe)]$^+$ (λ_{em}: 490 nm, Φ_{PL}: 18%, τ_e: 8.25 μs)[19b] (Fmppy = 2-[(4-fluorophenyl)-5-methyl]pyridinato); there is significant inconsistency in the reported properties of [(ppy)$_2$Ir-(dppe)]PF$_6$ with Lowry et al., quoting an emission maximum of 490 nm, a Φ_{PL} of 7.3% and a τ_e of 3.9 μs.[19b] None of this class of cationic complexes to date have been explored as emitters in solid-state lighting devices.

In the present work, we systematically study the properties of thirteen complexes of the form [Ir(C^N)$_2$(P^P)]PF$_6$ (Chart 1), with the bisphosphine ligand as one of six commonly used in the literature: xantphos, nixantphos, dpephos, dppe, Dppe and isopropxantphos, Scheme 1. In a bid to push the emission further into the blue and to enhance the photoluminescence quantum yield, a series of four C^N ligands were used: ppy, mesppy, dFppy and dFmesppy (mesppy = 2-phenyl-4-mesityl-pyridinato; dFmesppy = 2-(4,6-difluorophenyl)-4-mesitylpyridinato). The bulky mesppy and dFmesppy ligands were incorporated into the study as the latter had been previously shown by Bryce[22] and co-workers in [Ir(dFmesppy)$_2$(pic)] (pic = 2-piconilate) to (1) improve the solubility of the complex in organic solvents, which impacts positively homogeneous film deposition;[23] (2) promote reduced intermolecular interaction due to the bulky mesityl group and therefore reduced quenching phenomena, giving rise to increased Φ_{PL} in the solid state; (3) negligibly impact the emission energy, as the mesityl moiety is disposed in an nearly orthogonal and locked conformation with respect to the plane of the pyridine ring. Of all the bisphosphines, complexes with either dppe or Dppe as the ancillary ligand exhibited the highest photoluminescence quantum yield and longest emission lifetimes.

Eli Zysman-Colman

Eli Zysman-Colman obtained his Ph.D. from McGill University in 2003 under the supervision of Prof. David N. Harpp as an FCAR scholar where he conducting research in physical organic sulfur chemistry. He then completed two postdoctoral fellowships, one in supramolecular chemistry with Jay Siegel at the Organic Chemistry Institute, University of Zurich as an FQRNT fellow and the other in inorganic materials chemistry with Stefan Bernhard at Princeton University as a PCCM fellow. He joined the department of chemistry at the Université de Sherbrooke in Quebec, Canada as an assistant professor in 2007. In 2013, he moved to the University of St Andrews where he is an EaStCHEM Research Fellow/Lecturer (tenured). His research program focuses on the rational design of: (I) luminophores for energy-efficient visual displays and flat panel lighting based on organic light emitting diode (OLED) and light-emitting electrochemical cell (LEEC) device architectures; (II) light harvesting dyes for dye-sensitized solar cells (DSSCs) and organic photovoltaics; (III) sensing materials employed in electrochemiluminescence; and (IV) photoredox catalysts for organic reactions.

Results and discussion

Synthesis

The syntheses of the C^N ligands and the heteroleptic iridium complexes are shown in Scheme 1. Each of dFppy, mesppy and dFmesppy were prepared in high yield via Suzuki–Miyaura[24] palladium-catalysed cross-coupling reactions. The C^N ligands were complexed with IrCl$_3$·3H$_2$O and the resulting the μ-dichloro-bridged iridium dimers [Ir(ppy)$_2$Cl]$_2$, **D1**; [Ir(dFppy)$_2$Cl]$_2$, **D2**; [Ir(mesppy)$_2$Cl]$_2$, **D3**; and

This journal is © the Partner Organisations 2016

Inorg. Chem. Front., 2016, **3**, 218–235 | **219**

[Ir(dFmesppy)$_2$Cl]$_2$, **D4** were formed in good yield under standard conditions.[25] The iridium complexes **1–4** (Chart 1) were isolated in high yield through cleavage of **D1–D4** with the corresponding bisphosphine ligands: 4,5-bis-diphenylphosphino-9,9-dimethylxanthene (xantphos), **L$_a$**; bis(2-diphenylphosphinophenyl) ether (dpephos), **L$_b$**; 1,2-bis-(diphenylphosphino)ethene (dppe), **L$_c$**; 1,2-bis(diphenylphosphino)ethane (Dppe), **L$_d$**; 4,5-bis(diphenylphosphino)-9-isopropylenxanthene (isopropxantphos), **L$_e$**; and 2,4-bis-(diphenylphosphino)phenoxazine (nixantphos), **L$_f$**. All complexes were purified by column chromatography and isolated as the PF$_6^-$ salt following an anion metathesis reaction using NH$_4$PF$_6$. The purity of the complexes was confirmed by ^{1}H, ^{13}C, ^{19}F and ^{31}P NMR spectroscopy, HRMS and melting point

analyses (^{1}H, ^{13}C, ^{31}P, ^{19}F-NMR and HRMS spectra are reported in the ESI†). HRMS analysis showed in each case the diagnostic molecular ion peak. The ^{31}P NMR spectra showed one singlet between −15 and −25 ppm, corresponding to the two magnetically equivalent phosphorous atoms in the P^P ligand and one septet at around −150 ppm, characteristic of the PF$_6$ anion. The ^{19}F NMR spectra for **4a**, **4b**, **3c**, **4c** showed two singlets between −105 and −110 ppm corresponding to the two fluorine atoms present on each C^N ligand and a doublet at around −70, −80 ppm, characteristic to the six magnetically equivalent fluorine atoms coupled to the phosphorous nucleus of the PF$_6$ anion. In addition, crystal structures of **1a**, **2a**, **4a**, **1b**, **4b**, **1c**, **3c**, **4c**, **1e**, were obtained through single crystal X-ray analysis.
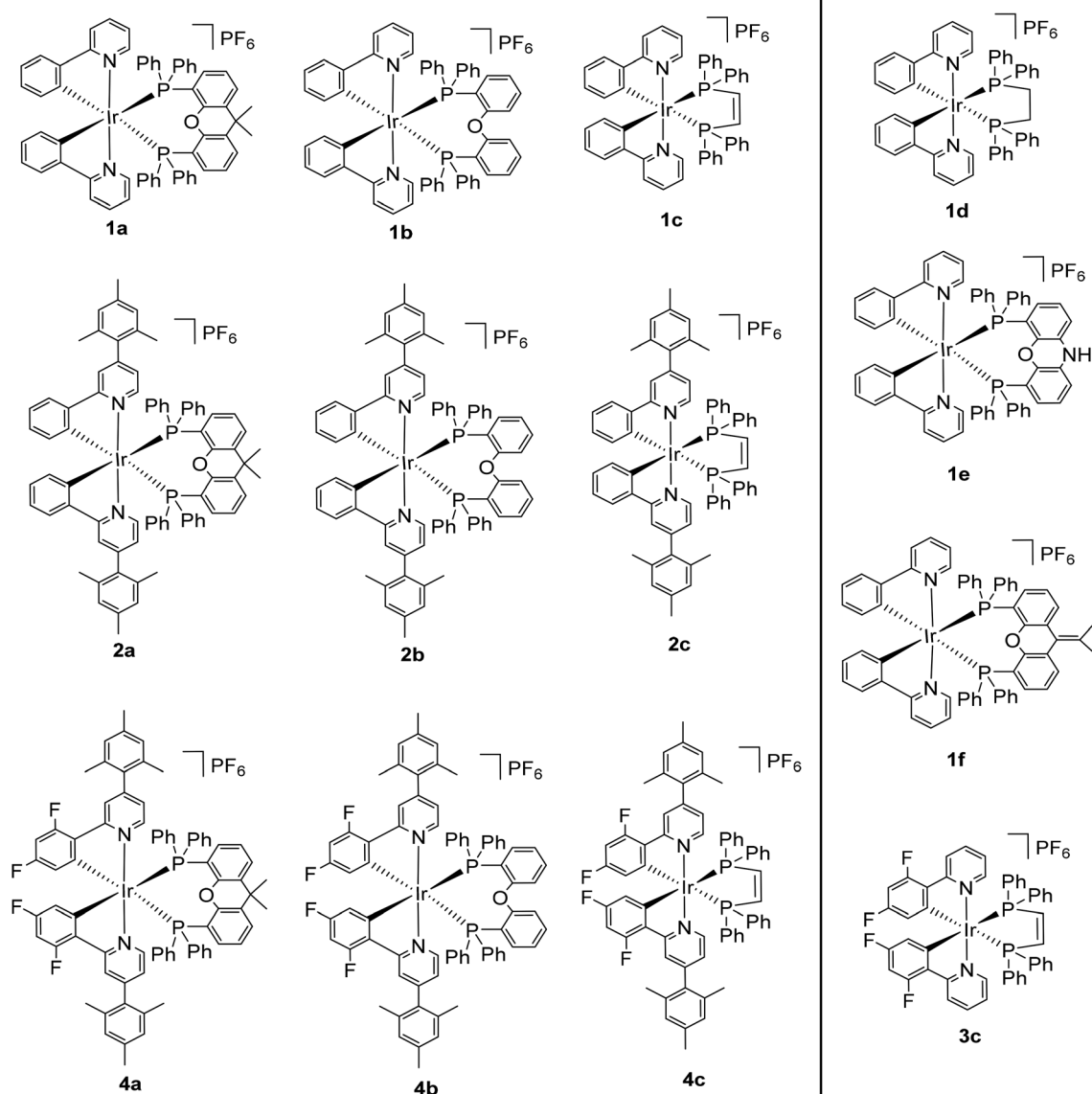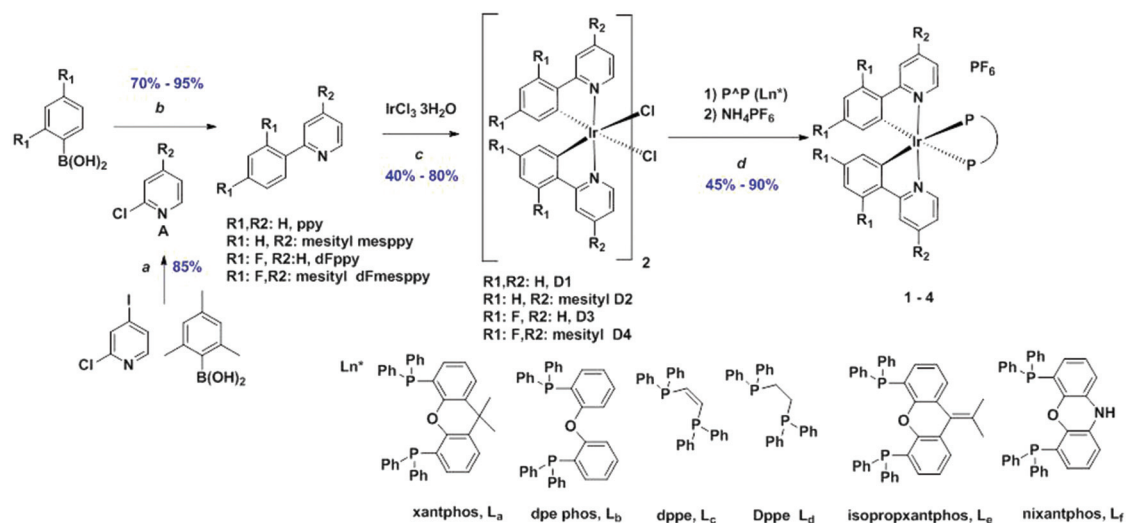

Chart 1 Chemical structure of complexes **1–4**.

220 | *Inorg. Chem. Front.*, 2016, **3**, 218–235

This journal is © the Partner Organisations 2016

Scheme 1 Synthesis of C^N ligands and [Ir(C^N)₂(P^P)]PF₆ complexes **1–4**. Reagents and conditions. [a]2.0 equiv. K_2CO_3, 5 mol% Pd(PPh₃)₄, N₂, 1,4-dioxane/H₂O (4 : 1 v/v), 105 °C, 56 h; [b]2.0 equiv. K_2CO_3, 5 mol% Pd(PPh₃)₄, N₂, 1,2-dimethoxyethane/H₂O (4 : 1 v/v), 130 °C, 19 h; [c]2-EtOC₂H₄OH/H₂O (4 : 1 v/v), 110 °C, N₂, 19 h. [d]i. CH₂Cl₂/MeOH (2 : 1 v/v), 55 °C, 19 h, N₂; ii. Excess solid NH₄PF₆.

Crystal structures

Crystal structures of complexes **1a**, **2a**, **4a**, **1b**, **4b**, **1c**, **3c**, **4c** and **1e** were obtained through X-ray diffraction studies. The structures of the Ir(III) complexes **1a**, **1b** and **1c** are shown in Fig. 1, those of complexes **4a**, **4b** and **4c** are shown in Fig. 2, whereas the remaining structures are reported in the ESI.†

In all the structures, the iridium centre adopts a distorted-octahedral geometry, as expected, with the two nitrogen atoms of the C^N ligands mutually *trans* to each other, and the two phosphorous atoms of the P^P ligand disposed *trans* with respect to the carbon atoms of the C^N ligands. Both the Ir–C and Ir–N bond lengths fall in the range expected for [Ir-(C^N)₂(L^L)] complexes (where L^L is any bidentate ligand),

and the Ir–P bond lengths also fall into the range expected for [Ir(C^N)₂(P^P)] complexes with two phosphorus donors (CSD version 5.36).[26] Those complexes with a mesityl-functionalized C^N ligand (**2a**, **4a**, **2b** and **4c**), all display the desired ortho-gonal orientation of the mesityl with respect to the pyridinato fragment The structures of **1b** and **1e** are closely related to those of the known structures of these complexes,[19a,c] including the arrangement of the complexes themselves. The differences primarily arise from changes in packing and solvation.

The P–Ir–P angles can be seen to vary in a systematic manner. For complexes **1a**, **2a** and **4a** (with xantphos), **1b** and **4b** (with dpephos) and **1e** (with nixantphos), the P–Ir–P bond angles are distorted to greater than 90° [angles varying between 98.74(7)° and 102.53(7)°]; whereas for complexes **1c**,
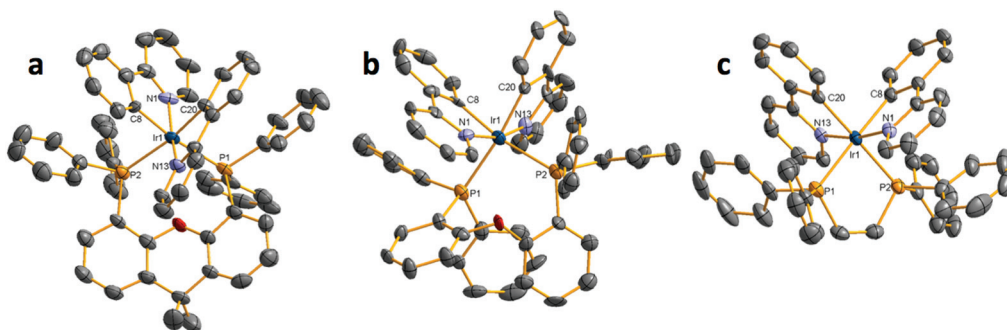

Fig. 1 Molecular structure of **1a** (a), **1b** (b) and **1c** (c). Hydrogen atoms, PF₆⁻ counterions, solvent molecules, minor components of disordered molecules and additional independent molecules are omitted for clarity. Selected bond lengths (Å) and angles (°): (**1a**) Ir₁–N₁ 2.079(6), Ir₁–N₁₃ 2.084(6), Ir₁–C₈ 2.042(7), Ir₁–C₂₀ 2.041(8), Ir₁–P₁ 2.482(2), Ir₁–P₂ 2.523(2), Ir₇₁–N₇₁ 2.074(6), Ir₇₁–N₈₃ 2.077(6), Ir₇₁–C₇₈ 2.051(7), Ir₇₁–C₉₀ 2.063(7), Ir₇₁–P₇₁ 2.483(2), Ir₇₁–P₇₂ 2.537(2), P₁–Ir₁–P₂ 102.53(7), P₇₁–Ir₇₁–P₇₂ 102.19(7); (**1b**) Ir₁–N₁ 2.092(10), Ir₁–N₁₃ 2.057(10), Ir₁–C₈ 2.022(13), Ir₁–C₂₀ 2.039(12), Ir₁–P₁: 2.448(4), Ir₁–P₂ 2.537(4), P₁–Ir₁–P₂ 99.53(12); (**1c**) Ir₁–N₁ 2.076(3), Ir₁–N₁₃ 2.072(3), Ir₁–C₈ 2.058(4), Ir₁–C₂₀ 2.059(4), Ir₁–P₁ 2.3680(11), Ir₁–P₂ 2.3593(11), Ir₅₁–N₅₁ 2.072(7), Ir₅₁–N₅₁ₐ 2.080(11), Ir₅₁–C₅₈ 2.060(5), Ir₅₁–P₅₁ 2.3558(13), P₁–Ir₁–P₂ 84.49(4), P₅₁–Ir₅₁–P₅₁(ₐ) 84.1(3). [Symmetry code: (A) −x + 1/2, y, 1 − z].

This journal is © the Partner Organisations 2016

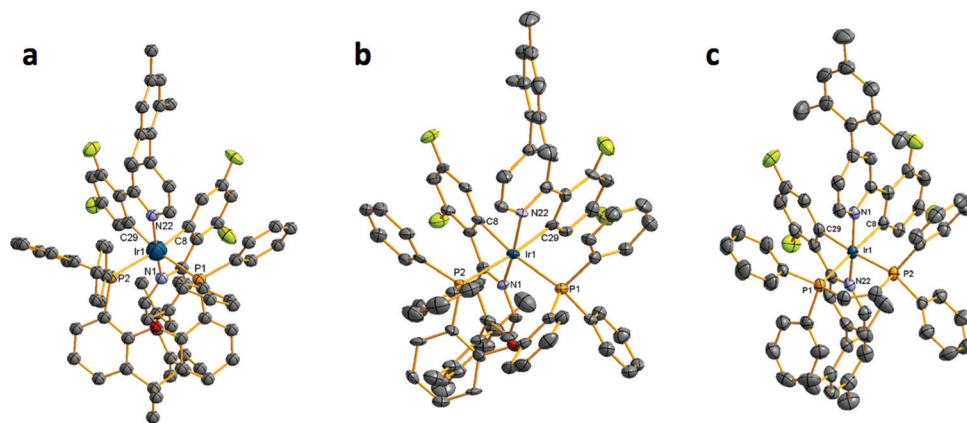*Inorg. Chem. Front.*, 2016, **3**, 218–235 | **221**

Fig. 2 Molecular structure of **4a** (a), **4b** (b) and **4c** (c). Hydrogen atoms, PF_6^- counterions, solvent molecules, minor components of disordered molecules and additional independent molecules are omitted for clarity. Selected bond lengths (Å) and angles (°): (**4a**) Ir_1–N_1 2.064(7), Ir_1–N_{22} 2.068(7), Ir_1–C_8 2.037(8), Ir_1–C_{29} 2.026(9), Ir_1–P_1 2.476(2), Ir_1–P_2 2.531(2), P_1–Ir_1–P_2: 100.81(8); (**4b**) Ir_1–N_1 2.084(6), Ir_1–N_{22} 2.068(6), Ir_1–C_8 2.061(8), Ir_1–C_{29} 2.052(8), Ir_1–P_1 2.461(2), Ir_1–P_2 2.473(2), P_1–Ir_1–P_2: 98.74(7); (**4c**) Ir_1–N_1: 2.063(2), Ir_1–N_{22} 2.067(3), Ir_1–C_8 2.053(3), Ir_1–C_{29} 2.064(3), Ir_1–P_1 2.3642(8), Ir_1–P_2 2.3653(8), P_1–Ir_1–P_2: 83.06(3).

3c and **4c** (with dppe) the P–Ir–P bond angles are reduced to less than 90° [angles varying between 83.06(3)° and 84.49(4)°]. This appears to arise from the size of the chelate formed by the P^P ligand, and its flexibility. In each of **1a**, **2a**, **4a**, **1b**, **4b** and **1e** an eight-membered chelate exists whereas in **1c**, **3c** and **4c** a more rigid five membered chelate is present. Additionally, the complexes with an eight-membered chelate break down into two sub-groups depending on the flexibility of the backbone of the P^P ligand, those complexes of xantphos and nixantphos showing a range of P–Ir–P bond-angles [100.81(8)–102.53(7)°] slightly above those seen in the more conformationally flexible dpephos complexes [98.74(7)–99.53(12)°]. To accommodate the varying sizes of chelate rings, the Ir–P bonds are found to vary in consequence, the complexes with smaller chelate rings showing shorter Ir–P bonds [2.3642(8)–2.3687(5) Å]

than those in the complexes with larger chelate rings [2.448(4)–2.537(2) Å].

Photophysical properties

The optoelectronic properties of complexes **1–4** have been investigated both in MeCN solution and in the solid state and are summarized in Table 1. The absorption spectra are shown in Fig. 3. The absorption spectra of all the complexes are characterized by two intense bands between 260 nm and 320 nm and a broad lower intensity band at around 360 nm. Similar to many other cationic iridium complexes of the form $[Ir(C^N)_2(P^P)]^+$ found in the literature,[16c,d,18,19] the two higher energetic bands can be attributed to the spin-allowed $^1\pi \rightarrow \pi^*$ ligand centered (^{1}LC) transitions localized on the C^N ligands, while the broad bands at wavelengths longer than 350 nm can

Table 1 Relevant photophysical data for **1–4**[a]

	λ_{em}[a,b] (nm)		Φ_{PL}[c] (%)		τ_e[a]	
	MeCN	Film[d]	MeCN	Film[d]	MeCN[e] (ns)	Film[d,e] (ns)
1a	484 [0.9], 510 [1]	507 [1], 657 [0.18]	0.3	0.8	6 (34.9), 20 (65.1)	5 (38.7), 40 (61.3)
2a	485 [0.90], 509 [1]	490 [0.90], 509 [1], 652 [0.18]	0.6	1.5	4 (18.7), 28 (81.3)	2 (23.0), 17 (22.8), 186 (54.2)
4a	461 [0.80], 489 [1]	474 [0.87], 500 [1], 630 [0.18]	0.7	5.7	17 (12), 36 (88)	50 (3.6), 306 (39.2), 882 (59.2)
1b	465 [0.80], 498 [1], 530 [0.60]	472 [0.65], 514 [1]	0.6	1.4	3 (5.9), 27 (94.0)	2 (16.3), 21 (17.2), 196 (66.5)
2b	466 [0.8], 501 [1], 539 [0.5]	472 [0.84], 504 [1], 538 [0.6]	0.9	1.7	4 (8.5), 28 (91.4)	3 (4.3), 44 (20.0), 303 (75.7)
4b	459 [0.82], 484 [1]	462 [0.82]; 486 [1]; 515 [0.70]	0.9	7.2	4 (9.5), 89 (90.4)	8 (10.6), 143 (19.1), 1070 (70.2)
1c	457 [0.95], 488 [1], 510 [0.58]	460 [0.56], 499 [1], 512 [0.92]	4.2	6.0	123 (2.7), 1105 (97.3)	6 (4.7), 150 (38.4), 1036 (56.9)
2c	456 [0.94], 486 [1], 516 [0.58]	462 [0.84], 492 [1], 517 [0.67]	4.5	7.8	5 (2.5), 1570 (97.5)	5 (2.9), 254 (14.2), 1183 (83.0)
4c	444 [0.78], 471 [1], 504 [0.63]	448 [0.77], 470 [1]; 504 [0.66]	52	37.2	179 (2.1), 13 468 (97.9)	3 (32.7), 245 (4.95), 3946 (62.38)
3c	445 [0.76], 471 [1], 503 [0.67]	446 [0.77], 472 [1], 500 [0.78]	18	20.7	25 (1.6), 9211 (98.7)	2 (30.2), 21 (5.6), 2598 (64.2)
1d	457 [0.95], 488 [1], 516 [0.59]	465 [0.37], 514 [1]	1.6	4.2	31 (1.7), 497 (98.2)	5 (6.1), 168 (30.0), 836 (64.0)
1f	485 [0.9], 509 [1]	478 [0.90], 499 [1], 598 [0.36]	0.6	0.7	6 (31.0), 26 (69.0)	1 (42.5), 12 (57.5)

[a] Measurements in degassed MeCN at 298 K. [b] Principal emission peaks listed with values in brackets indicating relative intensity. [c] Quinine sulfate employed as the external reference (Φ_{PL} = 54.6% in 0.5 M H_2SO_4 at 298 K).[29] [d] Films formed by dip-coating deposition on pristine quartz substrates. PLQY measurements were carried out under nitrogen. [e] Values in parentheses are pre-exponential weighting factor, in relative %, intensity, of the emission decay kinetics.

222 | *Inorg. Chem. Front.*, 2016, **3**, 218–235

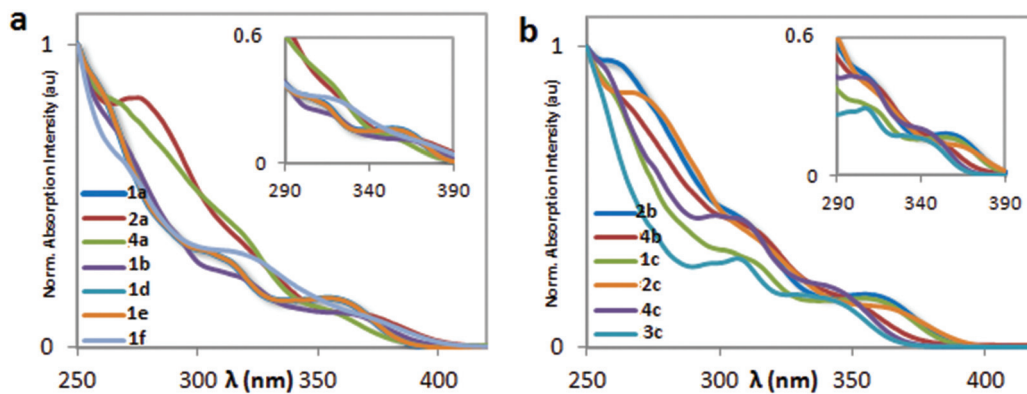This journal is © the Partner Organisations 2016

Fig. 3 UV-Vis spectra of complexes **1a**, **2a**, **4a**, **1b**, **1d**, **1e**, **1f** (a) and **2b**, **4b**, **1c**, **2c**, **4c**, **3c** (b) recorded in MeCN at 298 K.

be assigned to a mixture of spin-allowed and spin-forbidden metal-to-ligand charge transfer transitions (^{1}MLCT/^{3}MLCT). Indeed, as previously reported and predicted by TD-DFT calculations,[4a,27] spin-forbidden transitions directly to the triplet state are accessible in iridium(III) complexes due to the large spin–orbit coupling exhibited by the heavy iridium atom. The presence of the mesityl moiety in **2a**, **4a**, **2b**, **4b**, **2c** and **4c** leads to enhanced molar absorptivities in the UV region of the spectrum while also introducing a strongly absorbing shoulder at around 260–270 nm, the transition of which is assigned as ^{1}LC in nature.

Fig. 4 illustrates the normalized room temperate emission spectra of **1–4** upon photoexcitation into the $^1\pi \to \pi^*$ band (at 360 nm). Emission is blue to blue-green with emission maxima bunched between 460 nm and 510 nm. There are two distinct families of complexes based on their emission profiles. A structured vibronic emission profile is observed for **b**, **c** and **d** complexes (Fig. 4b) bearing one of dpephos, dppe and Dppe P^P ligands, which is indicative of a ^{3}LC excited state.[3c,11,19b,28] The emission is less structured for **1a**, **2a**, **4a**, **1f** (Fig. 4a) bearing xantphos-type ancillary ligands, which implicates greater ^{3}MLCT character.[19a,27a,e] No emission was detected for complex **1e**.

Incorporation of electron-withdrawing fluorine atoms on the C^N ligand promoted the expected stabilization of the frontier molecular orbitals and the blue-shift in the emission observed for complexes **4a**, **4b**, **4c** and **3c** compared with their fluorine-free congeners.[3b,20b]

Despite only minute variations in the emission energy, remarkable modulation of both Φ_{PL} and τ_e could be obtained through choice of C^N and P^P ligands. Firstly, of the ppy-containing complexes the highest photoluminescence quantum yields arise from complexes using dppe as the ancillary ligand (cf. **1c**), where Φ_{PL} at 4.2% is an order of magnitude higher than the other complexes in the series, save **1d**. Bi-exponential decay kinetics were observed for each of these complexes, similar to other [Ir(C^N)$_2$(P^P)]$^+$ complexes[19a] however, only in **1c** was there an observed microsecond component. Complex **1d**, bearing the Dppe P^P ligand, showed a modestly reduced Φ_{PL} of 1.2% and shorter bi-exponential decay (31 ns and 497 ns). Thus, the stronger bonding of the dppe (and Dppe) ligand to the iridium center has two effects: (1) there is a stron-
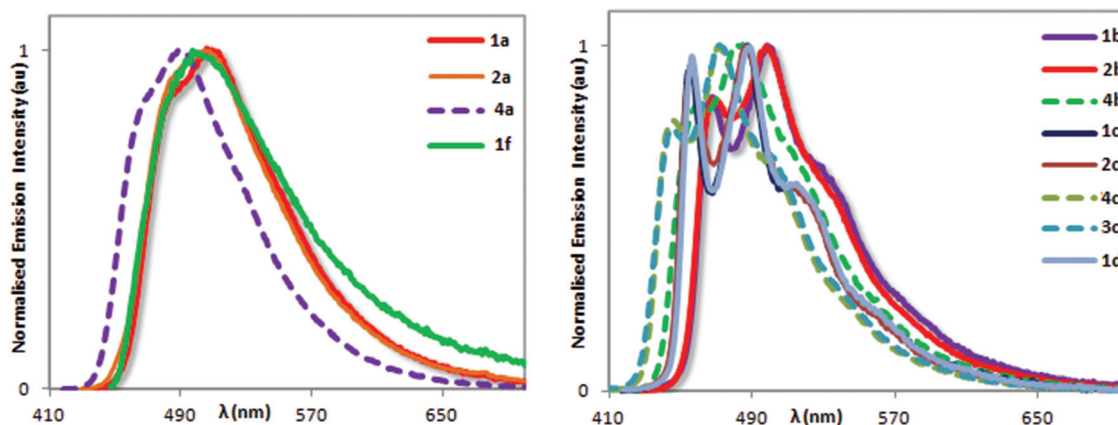

Fig. 4 Normalized photoluminescence spectra of complexes **1a**, **2a**, **4a**, **1f** (a) and **1b**, **2b**, **4b**, **1c**, **2c**, **4c**, **3c**, **1d** (b) recorded in degassed MeCN at 298 K (λ_{exc}: 360 nm).

This journal is © the Partner Organisations 2016

Inorg. Chem. Front., 2016, **3**, 218–235 | **223**

ger destabilization of the non-emissive MC states leading to an enhanced photoluminescence quantum yields and (2) there is a blue-shifted emission due to the stronger ligand field.[14–16,30]

In an effort to improve the Φ_{PL} of these complexes, we evaluated the family of mesppy-containing complexes (**2a**, **2b**, **2c**). Unfortunately only a slight improvement in the solution-state photophysical properties was observed. For instance, the Φ_{PL} for complex **2c**, [Ir(ppymes)$_2$(dppe)]PF$_6$, was 4.5% vs. 4.2% obtained for **1c**, [Ir(ppy)$_2$(dppe)]PF$_6$. Consistent with the energy gap law, along with the expected blue-shift in the solution-state emission (e.g., **3c**: λ_{em} = 471 nm; **1c**: λ_{em} = 488 nm) upon fluorine incorporation onto the C^N ligands, there is an observed enhanced photoluminescence quantum yield and longer emission lifetimes (e.g., **3c**: 18%; **1c**: 4.2%).[19a,b]

Considering the improved photophysical properties observed for **3c**, we decided to evaluate the family of dFmesppy cyclometalated complexes bearing xantphos, dpephos and dppe as ancillary ligands, with a view to reducing the intramolecular interactions and therefore the quenching phenomena following introduction of the bulky mesityl substituent.[22] Disappointingly, the observed Φ_{PL} and τ_e values for **4a** and **4b** remained essentially unaltered compared to analogs **2a** and **2b**. We were however delighted to observe the much-enhanced Φ_{PL} for **4c** at 52% and emission dominated by a component of lifetime of 13.5 μs compared to analog **3c**.

To discern if the effects observed in MeCN solution are transposable to the solid state, dip-coated neat films were analyzed. Generally, the trends observed in solution are mirrored in the films (Table 1), with slight enhancement in Φ_{PL}. It is worth noting that a remarkable improvement of the Φ_{PL} in the solid state was observed for **4a** and **4b**, which contain the dFmesppy C^N ligands. These two complexes are nearly non-emissive in MeCN (Φ_{PL}: 0.7% and 0.9%, respectively) with very short emission lifetimes (τ_e: ca. 36 ns and 89 ns, respectively) but significantly brighter in the solid state (Φ_{PL}: 5.7% and 7.4%, respectively and τ_e: ca. 882 ns and 1070 ns, respectively). Thus, the non-radiative pathways in solution that result from the flexibility of the eight-membered chelate of the P^P ligand are significantly mitigated as the complexes are rigidified in the solid state.

For **1b**, **1c** and **1d** bearing, respectively, dpephos, dppe and Dppe P^P ligands, a red shift in the emission energy (by up to 4.5×10^2 cm^{-1}) and broader emission are observed going from solution to the solid state (Fig. S77†). This is in agreement with many reports on aggregation phenomena of iridium(III) complexes in the solid state, in which either or both a red-shift in the emission and broadness in the emission bands is observed.[31] In order to overcome such effects, the ligands are often modified to incorporate bulky groups.[21i,31,32] Our results show that for **2b**, **4b**, **2c** and **4c** the bulky mesityl substituent suppresses aggregation in the solid state, with their thin film emission profiles mirroring those observed in MeCN solution. A similar, but less pronounced effect, is observed for complexes **1a** and **1f**, where the red-shifted emission in the solid state is noticeably reduced due to the bulkiness of the xantphos and isopropxantphos P^P ligands, respectively.

Electrochemical properties

The electrochemical properties of the complexes have been investigated by cyclic voltammetry in degassed MeCN and the oxidation potentials, E_{pa} (V), reported with respect to SCE (Fc/Fc$^+$ = 0.38 V in MeCN)[33] are compiled in Table S1.† For complexes bearing ppy and mesppy C^N ligands a single irreversible oxidation wave around 1.4 V is observed. When the complexes possess dFppy or dFmesppy C^N ligands, the oxidation potentials are more positive (E_{pa}: ca. 1.7 V) due to stabilization of the HOMO promoted by the fluorine electron-withdrawing substituents. Similar to other cationic iridium(III) complexes, these oxidation processes are assigned to the Ir^{III}/Ir^{IV} redox couple with significant involvement of the C^N ligands.[11,14] The absence of an observable reduction process within the solvent window points to a large electrochemical gap promoted by the strongly σ-donating P^P ligands.

Electroluminescent devices: light-emitting electrochemical cells (LEECs)

In view of the promising thin film photoluminescence properties of some of the ionic transition metal complexes (iTMC) in this study, light-emitting electrochemical cells (LEECs) based on compounds **1b**, **4a**, **4b** and **4c** were prepared, according to the procedure described in the Experimental section. LEECs consisted of a 100 nm thick emitting layer, sandwiched between an ITO/PEDOT:PSS (80 nm) anode (ITO = indium tin oxide; PEDOT:PSS = poly(3,4-ethylenedioxythiophene) polystyrene sulfonate) and a thermally evaporated aluminum cathode (70 nm) (Fig. 5c). The PEDOT:PSS layer was used to smoothen the ITO surface and hence to increase the yield and reproducibility of working devices. The device lifetime was measured by applying a pulsed current and by monitoring the voltage and luminance versus time, with a True Colour Sensor MAZeT (MTCSiCT Sensor) and a Botest OLT OLED Lifetime-Test System. The LEECs were driven using a pulsed current of 765 A m^{-2}, which is a high current density for this type of devices that leads to rapid degradation. The high current density, however, was necessary to increase the light emission to a level sufficient to be detectable by our equipment. All four LEECs showed a fast voltage drop at the initial operation stage, a consequence of fast ionic motion towards the electrode interfaces, which decreases the injection barrier for electrons and holes (see Fig. S99–102†).[34] Following the electrical double layers formation at the electrode interface, the injected charges create p- and n-doped regions in the active layer close to the correspondent electrode.[35] In spite of the typical electronic behavior of the LEECs, the luminance detected was rather low for all four devices. Assuming that electrons and holes are effectively injected into the active layer, the poor performance for the LEECs is attributed to the irreversibility of the phosphine ligand oxidation and to the high driving current density.

In a first attempt to exploit the potential of these new complexes, in view of their high photoluminescence efficiency, a host–guest LEEC was prepared using complex **4c** in the configuration as previously described,[36] which consisted on an

224 | Inorg. Chem. Front., 2016, **3**, 218–235

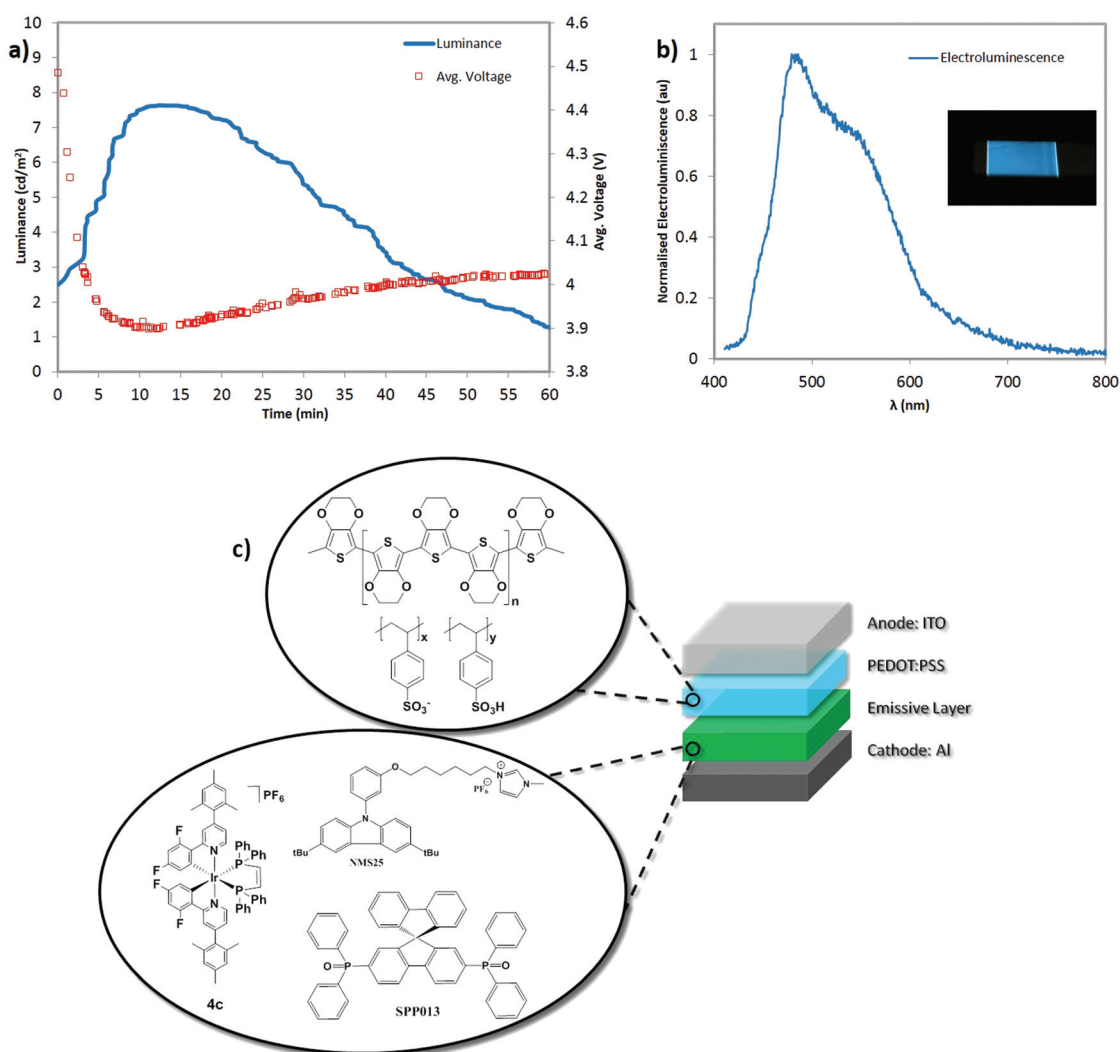This journal is © the Partner Organisations 2016

Fig. 5 (a) Luminance (solid blue line) and average voltage (open red squares) for ITO/PEDOT:PSS/active layer/Al (active layer = 1 : 1 by mass of NMS25 : SPPO13 with 10 wt% of **4c**) with a pulsed driving regime (block-wave pulsed current; 1000 Hz; 50% duty cycle; average density 100 A m^{-2}). (b) Electroluminescence spectrum with inset photo of LEEC. (c) Schematic representation of the LEEC architecture.

ionic carbazole (NMS25) and a spirobifluorene (SPPO13) as hole and electron transport materials, respectively. The host–guest layer was prepared using a NMS25 : SPPO13 mixture (1 : 1 mass ratio) doped with 10 wt% of **4c**. The host–guest device showed electroluminescence at a lower current density compared to the devices employing solely the iTMC (Fig. 5a). This is an indication of a better electronic transport through the host materials compared to the pure iTMC. The absolute electroluminescence of the host–guest system is somewhat low, which could be most likely due to an inadequate alignment of the lowest unoccupied molecular orbital (LUMO) of the iTMC with respect to the LUMO of the SPPO13 (−2.9 eV),[37] resulting in inefficient energy transfer from the host (SPPO13) to the guest (**4c**). The reduction wave in **4c** was found to lie outside the electrochemical window of the solvent (see electrochemistry section), which means that the LUMO energy of this material should be less than −2.8 eV (Fc/Fc$^+$ reference). The

host–guest LEEC showed a sky-blue electroluminescence, where the maximum emission corresponds to 479 nm (Fig. 5b).

We are currently working on the preparation of more suitable polar electron transport materials to attempt to improve these host guest devices.

Electroluminescent devices: organic light-emitting diodes (OLEDs)

OLEDs employing **3c** and **4c** were also fabricated and tested in light of their promising thin film photophysical properties. The device architecture consisted of the following structure: ITO/PEDOT:PSS (40 nm)/PVK (35 nm)/(mCP + Active layer + OXD7) (30 nm)]/B3PyMPM (60 nm)/Ca (20 nm)/Al (200 nm) structure, where **3c** or **4c** act as the active layer. PEDOT:PSS, PVK, mCP, OXD7 and B3PyMPM denote poly(3,4-ethylenedioxy-thiophene):poly(styrenesulfonate), poly(N-vinylcarbazole),

1,3-bis(*N*-carbazolyl)benzene, 2,2′-(1,3-phenylene)bis[5-(4-*tert*-butylphenyl)-1,3,4-oxadiazole] and bis-4,6-(3,5-di-3-pyridylphenyl)-2-methylpyrimidine, respectively (Fig. 6d). PVK facilitates the injection of holes and the electron transport layer B3PyMPM blocks the holes from penetration into cathode due to its deep lying HOMO and reduces the leakage current. Except for B3PyMPM and the contacts, all the layers were deposited by solution-processing methods. Device performance is summarized in Table 2.

The electroluminescence (EL) spectra are very similar to the PL spectra of the neat films as shown in Fig. 6a, an indication that in both cases the complexes are emitting from the same excited state. Fig. 6b shows the current-voltage-luminance characteristics of two devices. The turn-on voltages for both devices are similar. Fig. 6c shows the external quantum efficiency of the devices together with the power efficiency. Both the devices exhibit similar CIE coordinates (0.20, 0.29). Despite **4c** exhibiting a higher thin film Φ_{PL} compared to **3c** both OLED devices show similar poor efficiencies, which suggest that the performance of device 1 can be optimized further by improving the charge balance.

Conclusions

In summary, thirteen blue to blue-green emitting (λ_{em} 477–510 nm) cationic heteroleptic iridium(III) complexes bearing bisphosphine ancillary ligands have been synthesized and their optoelectronic properties investigated. Through optimization of the bite angle of the P^P chelate and introduction of bulky and fluorinated C^N ligands, we have rationally designed the brightest reported blue-emitting (λ_{em}: 471 nm) complex of this class in **4c** (Φ_{PL}: 52%). However, these complexes exhibit irreversible electrochemistry, which perhaps accounts for the poor LEEC performances observed using complexes **1b**, **4a**, **4b** and **4c**. The EL study shows that further refinement in charge balance is necessary in order to improve the performance of the OLED devices.

Experimental section

General synthetic procedures

Commercial chemicals were used as supplied. All reactions were performed using standard Schlenk techniques under inert (N_2) atmosphere with reagent grade solvents. Flash column chromatography was performed using silica gel (Silia-P from Silicycle, 60 Å, 40–63 μm). Analytical thin layer chromatography (TLC) was performed with silica plates with aluminum backings (250 μm with indicator F-254). Compounds were visualized under UV light. ^{1}H, ^{13}C, ^{31}P NMR ^{19}F NMR spectra were recorded on a Bruker Avance spectrometer at 500 MHz, 126 MHz and 471 MHz respectively. The following abbreviations have been used for multiplicity assignments: "s" for singlet, "d" for doublet, "t" for triplet, "m" for multiplet and "br" for broad. Deuterated chloroform (CDCl$_3$) and deuterated

dichloromethane (CD$_2$Cl$_2$) were used as the solvents of record. Melting points (Mp's) were recorded using open-ended capillaries on an Electrothermal melting point apparatus and are uncorrected. High-resolution mass spectra were recorded at the EPSRC UK National Mass Spectrometry Facility at Swansea University on a quadrupole time-of-flight (ESI-Q-TOF), model ABSciex 5600 Triple TOF in positive electrospray ionization mode and spectra were recorded using sodium formate solution as the calibrant.

Ligand syntheses

2-Chloro-4-(2,4,6-trimethylphenyl)pyridine (A). The synthesis of this ligand is by a modified method to a previously reported method.[22] 2-Chloro-4-Iodopyridine (4.0 g, 16.74 mmol), 2,4,6-trimethylphenyl boronic acid (4.0 g, 25.11 mmol), potassium carbonate (50 mmol) were added to a round bottomed flask containing 50 mL of a mixture of 1,4-dioxane and distilled water (4 : 1 v/v). The reaction mixture was degassed by multiple vacuum and N$_2$ purging cycles, and Pd(PPh$_3$)$_4$ (0.693 g, 0.60 mmol) was added to the flask under positive nitrogen pressure. The mixture was refluxed under nitrogen atmosphere for 48 h and then cooled to room temperature. The mixture was poured onto distilled water and extracted multiple times with dichloromethane. The organic fractions were combined, washed with a portion of brine and dried over magnesium sulfate. Filtration and evaporation under reduced pressure gave the crude product (3.80 g). The crude product was purified by flash column chromatography (5% ethyl acetate/hexane on silica) to give 3.30 g of pure compound as a colourless oil. Yield: 85%. R_f: 0.40 (20% EtOAc/hexanes on silica). ^{1}H NMR (500 MHz, CDCl$_3$) δ (ppm): 8.46 (d, J = 5.1 Hz, 1H), 7.18 (s, 1H), 7.06 (dd, J = 5.1, 1.4 Hz, 1H), 6.99 (s, 2H), 2.36 (s, 3H), 2.04 (s, 6H). The characterisation matches that reported.[22]

2-Phenyl-4-(2,4,6-trimethylphenyl)pyridine (mesppy). 2-Chloro-4-(2,4,6-trimethylphenyl)pyridine (**A**) (3.3 g, 14.24 mmol), phenyl boronic acid (2.78 g, 22.78 mmol), potassium carbonate (40 mmol) were added to a round bottomed flask containing 50 mL of a mixture of 1,2-dimethoxyethane and distilled water (4 : 1 v/v). The reaction mixture was degassed by multiple vacuum and N$_2$ purging cycles, and Pd(PPh$_3$)$_4$ (0.548 g, 0.48 mmol) was added to the flask under positive nitrogen pressure. The mixture was refluxed under nitrogen atmosphere for 19 h and then cooled to room temperature. The mixture was poured onto distilled water and extracted multiple times with dichloromethane. The organic fractions were combined, washed with a portion of brine and dried over magnesium sulfate. Filtration and evaporation under reduced pressure gave the crude product (3.90 g). The crude product was purified by flash column chromatography (silica, hexane/ethyl acetate gradient 100 : 0 to 80 : 20) to give 3.50 g of pure compound as a colourless oil. Yield: 87%. R_f: 0.38 (10% EtOAc/hexanes on silica). ^{1}H NMR (500 MHz, CDCl$_3$) δ (ppm): 8.77 (dd, J = 5.0, 0.8 Hz, 1H), 8.05 (m, 2H), 7.60 (q, J = 0.8 Hz, 1H), 7.54–7.42 (m, 3H), 7.09 (dd, J = 5.3, 1.3 Hz, 1H), 7.01 (s, 2H), 2.4 (s, 3H), 2.08 (s, 3H). ^{13}C NMR (126 MHz, CD$_2$Cl$_2$) δ (ppm):

226 | *Inorg. Chem. Front.*, 2016, **3**, 218–235

This journal is © the Partner Organisations 2016
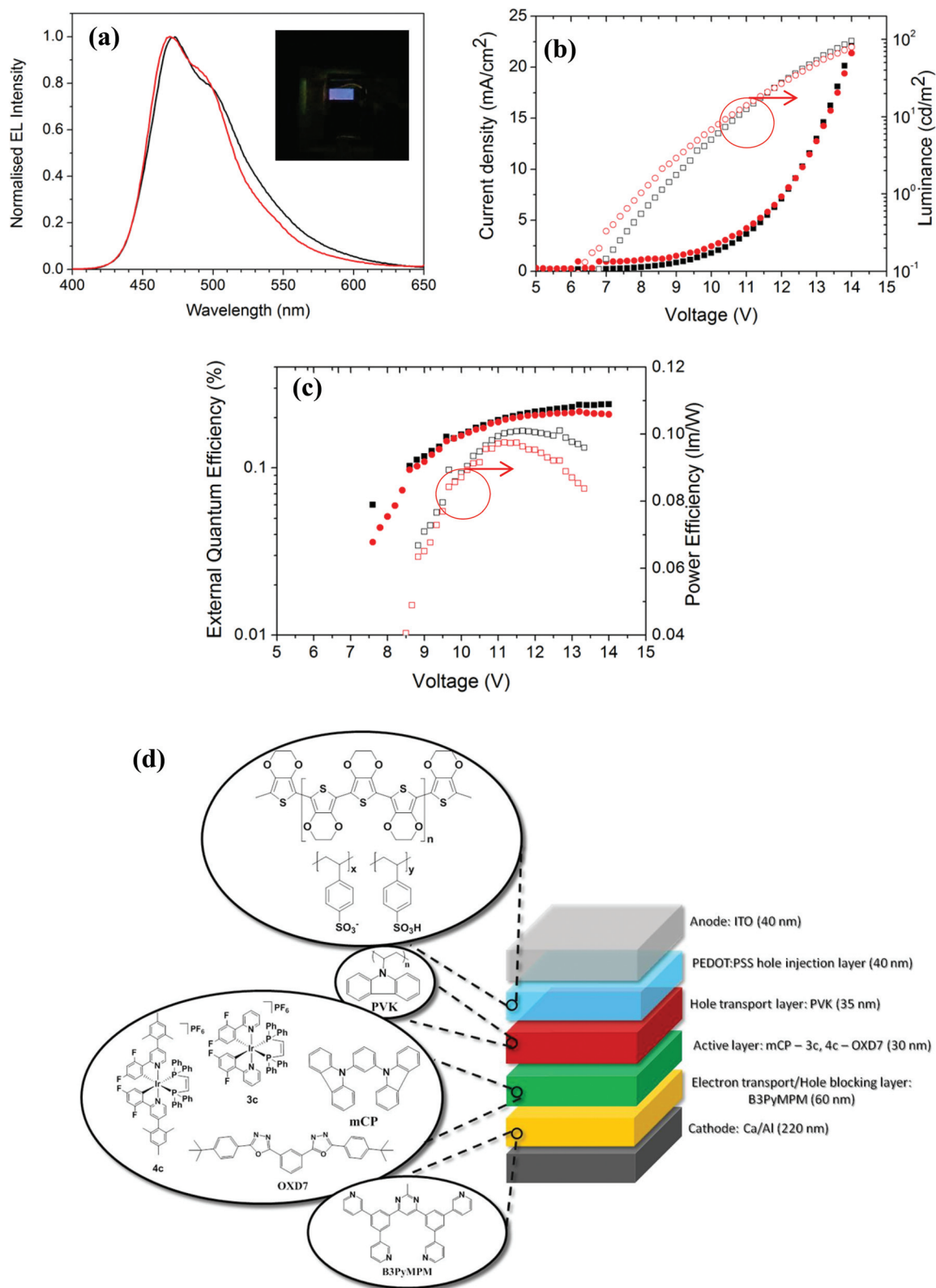
Fig. 6 (a) Normalized electroluminescent emission spectra of **4c** (black) and **3c** (red) in thin films. Inset shows the photograph of the working OLED with **4c**. (b) Current density and luminance *versus* applied voltage for OLEDs made with **4c** (black) and **3c** (red). (c) External quantum efficiency and Power efficiency *versus* applied voltage for OLEDs made with **4c** (black) and **3c** (red). (d) Schematic representation of the OLED architectures.

This journal is © the Partner Organisations 2016

Inorg. Chem. Front., 2016, **3**, 218–235 | **227**

Table 2 OLED performance data[a]

Device	Complex	Turn on voltage (V@ 1 cd m^{-2})	J (mA cm^{-2})	Luminance (cd m^{-2})	EQE (%)	PE (lm W^{-1})
1	**4c**	8.6	22.3	95.6	0.24	0.10
2	**3c**	8.0	21.2	79.9	0.21	0.09

[a] J = current density; EQE = external quantum efficiency; PE = power efficiency.

157.7, 150.3, 149.9, 139.4, 137.6, 136.5, 135.2, 129.1, 128.8, 128.6, 128.4, 127.0, 123.2, 121.5, 21.1, 20.7. FT-MS: Calculated: ($C_{20}H_{19}N$) 273.1585, found: 274.1585.

2-(2,4-Difluorophenyl)pyridine (dFppy). The synthesis of this ligand is by a modified method to a previously reported method.[6a] 2,4-Difluorophenylboronic acid (2.80 g, 17.70 mmol), 2-bromopyridine (2.00 g, 12.60 mmol), sodium carbonate (4.37 g, 31.60 mmol) were added to a round bottom flask containing a mixture of 1,4-dioxane and distilled water (4 : 1 v/v) to obtain a concentration of 0.15 to 0.20 M. The reaction mixture was degassed *via* bubbling nitrogen for 20 minutes. Pd(PPh$_3$)$_4$ (0.731 g, 0.633 mmol) was quickly added to the round bottom flask. The mixture was degassed again by evacuating and then backfilling with nitrogen three times, before heating to reflux. The mixture was refluxed under nitrogen atmosphere for 19 h, before cooling to room temperature and pouring onto distilled water. Extraction of the product with multiple portions of ethyl acetate was followed by combining the organic fractions, washing with water and then saturated sodium bicarbonate to remove residual boronic acid. Evaporation under reduced pressure gave the crude product. Purification by flash column chromatography (silica, hexane/ethyl acetate 95 : 5) gave 0.554 g of pure compound as a colourless oil. Yield: 70%. R_f: 0.48 (20% EtOAc/hexanes on silica). ^{1}H NMR (500 MHz, CDCl$_3$) δ (ppm): 8.72 (dt, J = 4.5 Hz, 1.0 Hz, 1H), 8.03–7.99 (m, 1H), 7.75 (d, J = 4.0 Hz, 2H), 7.28–7.23 (m, 1H), 7.03–6.99 (m, 1H), 6.93–6.90 (m, 1H). ^{13}C NMR (126 MHz, CDCl$_3$) δ (ppm): 164.6, 162.1, 159.5, 152.7, 149.9, 136.6, 132.3, 124.4, 122.6, 112.1, 104.5. ^{19}F {^{1}H} NMR (471 MHz, CDCl$_3$) δ (ppm): −109.3 (d, J = 6.8 Hz, 1F), −113.0 (d, J = 6.8 Hz, 1F). GCMS: (13.6 min) [M]$^+$: 191. The characterisation matches that reported.[6a]

2-(2,4-Difluorophenyl)-4-(2,4,6-trimethylphenyl)pyridine (dFmesppy). The synthesis of this ligand is by a modified method to that previously reported.[22] 2-Chloro-4-(2,4,6-tri-methylphenyl)pyridine (A) (2.28 g, 9.88 mmol), 2,4-Difluorphe-nylphenyl boronic acid (2.18 g, 13.82 mmol), potassium carbonate (3.41 g, 24.51 mmol) were added to a Schlenk tube containing a mixture of 1,2-dimethoxyethane and distilled water (4 : 1 v/v). The reaction mixture was degassed by multiple vacuum and N$_2$ purging cycles, and Pd(PPh$_3$)$_4$ (0.571 g, 0.494 mmol) was added to the tube under positive nitrogen pressure. The mixture was refluxed under nitrogen atmosphere

for 19 h and then cooled to room temperature. The mixture was poured onto distilled water and extracted multiple times with dichloromethane. The organic fractions were combined, washed with a portion of brine and dried over magnesium sulfate. Filtration and evaporation under reduced pressure gave the crude product (3.59 g). The crude product was puri-fied by flash column chromatography (silica, hexane/ethyl acetate 9 : 1) to give 2.88 g of pure compound as a colourless oil. Yield: 94%. R_f: 0.43 (hexane/ethyl acetate, 6 : 1 on silica). ^{1}H NMR (500 MHz, CDCl$_3$) δ (ppm): 8.75 (dd, J = 7.5 Hz, 1.5 Hz, 1H), 8.08 (dt, J = 8.5, 10 Hz, 1H), 7.59 (m, 1H), 7.09 (dd, J = 5.0 Hz, 1.5 Hz, 1H), 7.02 (tdd, J = 10.0, 3.3, 1.0 Hz, 1H) 6.97 (d, J = 1.0 Hz, 2H), 6.90 (dt, J = 3.0, 12.5 Hz, 1H), 2.34 (s, 3H), 2.05 (s, 6H). ^{13}C NMR (126 MHz, CDCl$_3$) δ (ppm): 164.67, 161.97, 159.45, 152.85, 122.83, 150.16, 150.05, 137.78, 136.39, 135.37, 132.40, 132.36, 132.30, 132.26, 128.53, 125.48, 125.38, 123.67, 112.15, 112.12, 111.94, 111.91, 104.80, 104.54, 104.28, 21.20, 20.76. ^{19}F {^{1}H} NMR (471 MHz, CDCl$_3$) δ (ppm): −109.3 (d, J = 9.4 Hz, 1F), −112.7 (d, J = 9.4 Hz, 1F). HR-MS (APCI$^+$): [M + H]$^+$ Calculated: ($C_{20}H_{17}F_2NH$) 310.1402; Found: 310.1402. The characterisation matches that reported.[22]

General procedure for the synthesis of [(C^N)$_2$Ir]$_2$Cl$_2$ dimers

The iridium(III) dimers, [(ppy)$_2$Ir(μ-Cl)]$_2$, [(mesppy)$_2$Ir(μ-Cl)]$_2$, [(dFppy)$_2$Ir(μ-Cl)]$_2$ [(dFmesppy)$_2$Ir(μ-Cl)]$_2$ were prepared accord-ing to the procedure described by Nonoyama.[25] Briefly, to a round bottomed flask containing IrCl$_3$·3H$_2$O (1.0 equiv.) and C^N ligand (2.2 equiv.) was added 2-ethoxyethanol to give a concentration of 0.02 M. The reaction mixture was degassed by multiple vacuum and N$_2$ purging cycles and the mixture was heated to reflux at 120 °C for 19 h. The solution was cooled to room temperature and the yellow precipitate was filtered, washed with water, hexane and ether and finally dried under vacuum to afford the pure material.

Tetrakis[2-(4′,6′-difluorophenyl)-4-(2,4,6-trimethylphenyl)-pyridinato-N,C$^{2'}$]-bis(μ-chloro)diiridium(III) [Ir(mesppy)$_2$-(μ-Cl)]$_2$ (D2). Yield: 70%. ^{1}H NMR (500 MHz, CD$_2$Cl$_2$) δ (ppm): 9.69 (d, J = 6.4 Hz, 2H), 7.77 (s, 4H), 7.55 (d, J = 9.0 Hz, 4H), 7.05 (d, J = 10.9 Hz, 8H), 6.86 (m, 7H), 6.72 (dt, J = 8.1 Hz, 4H), 5.95 (d, J = 8.1 Hz, 4H), 2.42 (s, 12H), 2.16 (s, 12H), 2.15 (s, 12H).

Tetrakis[2-(4′,6′-difluorophenyl)-pyridinato-N,C$^{2'}$]-bis(μ-chloro)-diiridium(III), [Ir(dFppy)$_2$(μ-Cl)]$_2$ (D3). Yield: 46%. ^{1}H NMR (500 MHz, CD$_2$Cl$_2$) δ (ppm): 9.12 (d, J = 5.0 Hz, 4H), 8.33 (d, J = 8.5 Hz, 4H), 7.88 (t, J = 7.0 Hz, 4H), 6.87 (td, J = 5.8, 1.0 Hz, 4H), 6.38 (td, J = 11.0, 2.0 Hz, 4H) 5.31 (dd, J = 9.3 Hz, 2.0 Hz, 4H). ^{19}F {^{1}H} NMR (471 MHz, CD$_2$Cl$_2$) δ (ppm): −108.4 (d, J = 9.4 Hz, 4F), −110.6 (d, J = 9.4 Hz, 4F).

Tetrakis[2-(4′,6′-difluorophenyl)-4-(2,4,6-trimethylphenyl)-pyridinato-N,C$^{2'}$]-bis(μ-chloro)diiridium(III), [Ir(dFmesppy)$_2$-(μ-Cl)]$_2$ (D4). Yield: 81%. ^{1}H {^{19}F} NMR (400 MHz, CD$_2$Cl$_2$) δ (ppm): 9.57 (d, J = 6.0 Hz, 4H), 8.13 (s, 4H), 7.02 (d, J = 10.4 Hz, 8H), 6.89 (dd, J = 6.0, 2.0 Hz, 4H), 5.29 (m, 4H) 2.38 (s, 12H), 2.12 (s, 24H). ^{19}F {^{1}H} NMR (371 MHz, CD$_2$Cl$_2$) δ (ppm): −108.1 (d, J = 11.1 Hz, 4F), −110.2 (d, J = 10.8 Hz, 4F).

228 | *Inorg. Chem. Front.*, 2016, **3**, 218–235

This journal is © the Partner Organisations 2016

General procedure for the synthesis of [Ir(C^N)$_2$(P^P)]PF$_6$ complexes

To a Schlenk tube containing [Ir(ppy)$_2$Cl]$_2$, (**D1**), [Ir(mesppy)$_2$Cl]$_2$ (**D2**), ([Ir(dFppy)$_2$Cl]$_2$, (**D3**) or [Ir(dFmesppy)$_2$Cl]$_2$, (**D4**) (1.0 equiv.) and P^P ligand (2.5 equiv.) were added DCM and MeOH (2 : 1 v/v) to give a concentration of 0.03 M. The reaction mixture was degassed by multiple vacuum and N$_2$ purging cycles and the mixture and the mixture was heated to 55 °C for 19 h under nitrogen atmosphere. The solution was cooled to room temperature and solid NH$_4$PF$_6$ (10.0 equiv.) was added and the reaction mixture was left to stir for a further 1 h. The resulting suspension was evaporated to dryness, with the residue then copiously washed with Et$_2$O and distilled water. This crude product was purified by flash column chromatography (silica, DCM/MeOH gradient 100 : 0 to 90 : 10). Fractions containing the desired complex were combined and solid NH$_4$PF$_6$ (10 equiv.) was added. The suspension was stirred at room temperature for 0.5 h. This mixture was then evaporated to dryness, washed vigorously with distilled water and dried to afford the pure material.

Iridium(III)bis[2-phenylpyridinato]-4,5-bis(diphenylphosphino)-9,9-dimethylxanthenehexafluorophosphate, [Ir(ppy)$_2$(xantphos)]-(PF$_6$) (1a). Yield: 73%. R_f: 0.24 (DCM + 3% MeOH). Mp: 292–302 °C (degraded). ^{1}H NMR (500 MHz, CDCl$_3$) δ (ppm): 8.61 (d, J = 5.7 Hz, 2H), 7.88 (d, J = 4.1 Hz, 4H), 8.5 (dd, J = 1.3, 7.6 Hz, 2H), 7.32–7.31 (m, 4H), 7.12–7.07 (m, 7H), 6.84 (m, 8H), 6.78 (m, 2H), 6.71 (m, 2H), 6.64 (t, J = 7.4 Hz, 2H), 6.42 (t, J = 8.4 Hz, 4H), 6.28 (t, J = 7.8 Hz, 2H), 5.20 (d, J = 7.9 Hz, 2H), 1.15 (s, 3H), 1.13 (s, 3H). ^{13}C NMR (126 MHz, CDCl$_3$) δ (ppm): 154.44, 141.66, 138.79, 134.11, 134.03, 132.36, 131.12, 130.94, 129.87, 129.61, 129.52, 128.53, 128.02, 125.12, 125.10, 124.15, 123.58, 122.90, 120.32, 109.99, 30.97, 29.59, 22.88 ppm. ^{31}P NMR (162 MHz, CDCl$_3$) δ (ppm): −20.2, −145.0 (hept). HR NSI$^+$ MS: [M − PF$_6$]$^+$ Calculated: (C$_{61}$H$_{48}$IrN$_2$OP$_2$): 1079.2871; Found: 1079.2856. The characterization matches that reported.[19a]

Iridium(III)bis[2-phenyl-4-(2,4,6-trimethylphenyl)pyridinato]-4,5-bis(diphenylphosphino)-9,9-dimethylxanthene hexafluorophosphate, [Ir(mesppy)$_2$(xantphos)](PF$_6$) (2a). Yield: 89%. R_f: 0.28 (DCM + 3% MeOH). Mp: 234–237 °C. ^{1}H NMR (500 MHz, CD$_2$Cl$_2$) δ (ppm): 8.76 (d, J = 5.9 Hz, 2H), 7.70 (s, 2H), 7.60 (d, J = 7.0 Hz, 2H), 7.31 (t, J = 7.6 Hz, 2H), 7.30 (d, J = 8.0 Hz, 2H), 7.15 (m, 9H), 6.95 (m, 14H), 6.70 (t, J = 6.8 Hz, 2H), 6.63 (t, J = 6.8 Hz, 4H), 6.58 (dd, J = 1.5, 6.1 Hz, 2H), 6.30 (t, J = 6.9 Hz, 2H), 5.16 (d, J = 7.9 Hz, 2H), 2.36 (s, 6H), 2.01 (s, 6H), 1.49 (s, 6H). ^{13}C NMR (126 MHz, CD$_2$Cl$_2$) δ (ppm): 154.17, 138.66, 134.08, 132.63, 132.59, 131.22, 131.16, 129.72, 129.65, 128.71, 128.51, 128.38, 128.19, 128.01, 127.11, 125.10, 124.93, 124.16, 122.86, 121.89, 29.68, 28.57, 20.88, 20.81, 20.11. ^{31}P NMR (162 MHz, CD$_2$Cl$_2$) δ (ppm): −20.13, −144.41 (hept). HR NSI$^+$ MS: [M − PF$_6$]$^+$ Calculated: (C$_{79}$H$_{68}$IrN$_2$OP$_2$): 1315.4436; Found: 1315.4419.

Ir(III)bis[2-(2,4-difluoro)-phenyl-4-(2,4,6-trimethylphenyl)pyridinato]-4,5-bis(diphenylphosphino)-9,9-dimethylxanthene hexafluorophosphate, [Ir(dFmesppy)$_2$(xantphos)](PF$_6$) (4a). Yield:

89%. R_f: 0.25 (DCM + 5% MeOH). Mp: 234–238 °C. ^{1}H NMR (500 MHz, CD$_2$Cl$_2$) δ (ppm) 8.85 (d, J = 5.5 Hz, 2H), 8.15 (s, 2H), 7.69 (d, J = 6.8 Hz, 2H), 7.48 (t, J = 7.9 Hz, 2H), 7.28 (t, J = 7.1 Hz, 6H), 7.22 (t, J = 7.1 Hz, 3H), 7.05 (m, 17H), 6.75 (t, J = 7.3, 4H), 6.68 (dd, J = 5.6, 1.9 Hz, 2H), 6.22 (dt, J = 7.4, 1.2 Hz, 2H), 2.39 (s, 6H), 2.15 (s, 6H), 2.03 (s, 6H), 1.57 (s, 6H), 1.53 (s, 6H). ^{13}C NMR (126 MHz, CD$_2$Cl$_2$) δ (ppm): 164.80, 154.15, 153.91, 153.09, 138.82, 134.71, 134.23, 134.09, 133.85, 132.69, 132.51, 131.26, 130.29, 128.95, 128.82, 128.61, 128.20, 125.82, 125.64, 125.39, 116.86, 112.57, 112.42, 99.16, 28.77, 20.82, 20.11. ^{19}F NMR (162 MHz, CD$_2$Cl$_2$) δ (ppm): −72.8, −74.4, −104.5, −108.5. ^{31}P NMR (162 MHz, CD$_2$Cl$_2$) δ (ppm) −20.13, −145.23 (hept). FT NSI$^+$ MS: [M − PF$_6$]$^+$ Calculated (C$_{79}$H$_{64}$F$_4$IrN$_2$OP$_2$): 1387.4059; Found: 1357.4041.

Iridium(III)bis[2-phenylpyridinato]-bis[(2-diphenylphosphino)-phenyl]methane hexafluorophosphate, [Ir(ppy)$_2$(dpephos)](PF$_6$) (1b). Yield: 48%. R_f: 0.21 (DCM + 3% MeOH). Mp: 291–299 °C (degraded). ^{1}H NMR (500 MHz, CD$_2$Cl$_2$) δ (ppm): 8.76 (d, J = 6.4 Hz 2H), 7.70 (t, J = 8.0 Hz, 2H), 7.57 (d, J = 8.0 Hz, 2H), 7.16 (t, J = 8.5, 2H), 7.30–7.11 (m, 20H), 7.06 (t, J = 7.1 Hz, 2H), 6.92 (t, J = 7.2 Hz, 4H), 6.80–6.72 (m, 4H), 6.66 (m, 2H), 6.48–6.39 (m, 6H), 5.35 (dd, J = 8.4 Hz, 2H). ^{13}C NMR (126 MHz, CD$_2$Cl$_2$) δ (ppm): 166.60, 152.87, 140.85, 136.46, 133.22, 130.09, 128.48, 127.15, 126.03, 123.25, 123.33, 121.33, 120.84, 118.11, 117.09. ^{31}P NMR (162 MHz, CD$_2$Cl$_2$) δ (ppm): δ −15.98, −145.23 (hept). HR NSI$^+$ MS: [M − PF$_6$]$^+$ Calculated: (C$_{58}$H$_{44}$IrN$_2$OP$_2$): 1039.2558; Found: 1039.2543. The characterization matches that reported.[19c]

Iridium(III)bis[2-phenyl-4-(2,4,6-trimethylphenyl)pyridinato]-bis[(2-diphenylphosphino)phenyl]methane hexafluorophosphate, [Ir(mesppy)$_2$(dpephos)](PF$_6$) (2b). Yield: 83%. R_f: 0.27 (DCM + 3% MeOH). Mp 234–236 °C. ^{1}H NMR (500 MHz, CD$_2$Cl$_2$) δ (ppm): 8.86 (d, J = 5.2 Hz, 2H), 7.48 (s, 2H), 7.38–7.32 (m, 6H), 7.27 (q, J = 8.4 Hz, 4H), 7.20 (t, J = 7.5 Hz, 8H), 7.12 (t, J = 9.3 Hz, 2H), 7.02–6.97 (m, 8H), 6.82 (t, J = 6.8 Hz, 2H), 6.70 (d, J = 10.1 Hz, 2H), 6.59–6.51 (m, 8H), 5.39 (d, J = 6.2 Hz, 2H), 2.34 (s, 6H), 2.03 (s, 12H), 1.97 (s, 6H). ^{13}C NMR (126 MHz, CD$_2$Cl$_2$) δ (ppm): 154.58, 135.32, 135.24, 132.86, 132.72, 132.23, 130.56, 130.29, 129.94, 129.23, 128.67, 128.43, 128.36, 127.82, 125.16, 124.33, 124.25, 123.23, 121.78, 118.97, 20.78, 20.13, 0.75. ^{31}P NMR (162 MHz, CD$_2$Cl$_2$) δ (ppm): −16.09, −145.23 (hept). HR NSI$^+$ MS: [M − PF$_6$]$^+$ Calculated: (C$_{76}$H$_{64}$IrN$_2$OP$_2$): 1275.4123; Found: 1275.4121.

Iridium(III)bis[2-(2,4-difluorophenyl)-4-(2,4,6-trimethylphenyl)-pyridinato]-bis[(2-diphenylphosphino)phenyl]methane hexafluorophosphate, [(dFmesppy)$_2$Ir(dpephos)](PF$_6$) (4b). Yield: 85%. R_f: 0.22 (DCM + 5% MeOH). Mp: 303–306. ^{1}H NMR (500 MHz, CD$_2$Cl$_2$) δ (ppm) 8.92 (d, J = 6.4 Hz, 2H), 7.90 (s, 2H), 7.45–7.13 (m, 20H), 7.10 (t, J = 6.8, 4H), 7.00 (d, J = 12.8 Hz, 4H), 6.74 (d, J = 5.5 Hz, 2H), 6.67 (t, J = 8.6 Hz, 3H), 6.61 (dd, J = 6.1, 1.1 Hz, 2H), 6.38 (dt, J = 9.6 Hz, 1.5 Hz, 2H), 2.34 (s, 6H), 2.03 (s, 6H), 1.96 (s, 6H). ^{13}C NMR (126 MHz, CD$_2$Cl$_2$) δ (ppm) 164.79, 156.63, 154.62, 153.44, 138.68, 135.07, 134.76, 134.16, 133.38, 132.78, 132.09, 130.97, 129.35, 128.68, 128.02, 127.41, 125.50, 125.29, 124.74, 119.07, 112.91, 99.72, 65.67, 20.79, 20.15. ^{19}F NMR (162 MHz, CD$_2$Cl$_2$) δ (ppm):

This journal is © the Partner Organisations 2016

Inorg. Chem. Front., 2016, **3**, 218–235 | **229**

−72.8, −74.4, −106.4, −108.4. ^{31}P NMR (162 MHz, CD$_2$Cl$_2$) δ (ppm): −17.66, −145.23 (hept). FT NSI$^+$ MS: [M − PF$_6$]$^+$ Calculated: (C$_{70}$H$_{60}$F$_4$IrN$_2$OP$_2$): 1347.3746; Found: 1347.3731.

Iridium(III)bis[2-phenylpyridine]-Bis[1,2-bis(diphenylphosphino)-ethenato] hexafluorophosphate, [Ir(ppy)$_2$(dppe)](PF$_6$) (1c). Yield: 78%. R_f: 0.23 (DCM + 3% MeOH). Mp: 331–335 °C. ^{1}H NMR (500 MHz, CD$_2$Cl$_2$) δ (ppm): 8.42 (dd, J = 52 Hz, 2H), 7.77 (t, J = 8 Hz, 4H), 7.54 (d, J = 4.2 Hz, 2H), 7.51 (t, J = 4.2, 2H), 7.50 (t, J = 8 Hz, 4H), 7.45 (t, J = 8.3 Hz, 6H), 7.12 (t, J = 4.1 Hz, 2H), 7.07 (t, J = 5.1 Hz, 2H), 7.02 (t, J = 4.4 Hz, 2H), 6.88 (t, J = 8.5 Hz, 4H), 6.51 (t, J = 8 Hz, 4H), 6.32 (m, 4H), 1.27 (s, 2H). ^{13}C NMR (126 MHz, CD$_2$Cl$_2$) δ (ppm): 167.49, 152.99, 152.96, 148.88, 148.62, 148.34, 143.26, 137.65, 132.69, 132.66, 132.62, 131.82, 130.36, 129.73, 129.63, 129.60, 129.56, 129.46, 129.42, 128.42, 128.34, 125.12, 123.64, 122.90, 120.18. ^{31}P NMR (162 MHz, CD$_2$Cl$_2$) δ (ppm): −20.86, −145.23 (hept). HR NSI$^+$ MS: [M − PF$_6$]$^+$ Calculated: (C$_{48}$H$_{38}$IrN$_2$P$_2$): 897.2139; Found: 897.2121. The characterization matches that reported.^{19d}

Iridium(III)bis[2-phenyl-4-(2,4,6-trimethylphenyl)pyridinato]-bis[1,2-bis(diphenylphosphino)ethene] hexafluorophosphate, [Ir(mesppy)$_2$(dppe)](PF$_6$) (2c). Yield: 88%. R_f: 0.28 (DCM + 3% MeOH). Mp 230–235 °C. ^{1}H NMR (500 MHz, CD$_2$Cl$_2$) δ (ppm): 8.59 (dd, J = 50 Hz, 2H), 7.84 (t, J = 7.7 Hz, 4H), 7.52 (d, J = 9.8 Hz, 2H), 7.50 (d, J = 10.2, 2H), 7.48 (m, 6H), 7.43 (d, J = 2.3 Hz, 2H), 7.11 (t, J = 6.1 Hz, 2H), 7.05 (q, J = 15.6, 4H), 7.00 (t, J = 9.8 Hz, 4H), 6.97 (m, 4H), 6.72 (t, J = 10.25 Hz, 4H), 6.24 (dd, J = 5.4 Hz, 4H), 6.19 (dd, J = 4.8 Hz, 2H), 1.97 (s, 6H), 1.85 (s, 6H), 1.27 (s, 6H). ^{13}C NMR (126 MHz, CD$_2$Cl$_2$) δ (ppm): 173.80, 132.51, 131.81, 131.58, 130.42, 130.28, 129.72, 129.69, 129.53, 128.39, 125.18, 122.14, 123.77, 121.64, 83.41, 80.11, 20.74, 20.05. ^{31}P NMR (162 MHz, CD$_2$Cl$_2$) δ (ppm): −19.71, −145.23 (hept). HR NSI$^+$ MS: [M − PF$_6$]$^+$ Calculated (C$_{66}$H$_{58}$IrN$_2$P$_2$): 1133.3704; Found: 1133.3695.

Iridium(III)bis[2-(2,4-difluorophenyl)-4-(2,4,6-trimethylphenyl)-pyridinato]-bis[1,2-bis(diphenylphosphino)ethene] hexafluoro-phosphate, [Ir(dFmesppy)$_2$(dppe)](PF$_6$) (4c). Yield: 88%. R_f: 0.30 (DCM + 5% MeOH). Mp: 369–372 °C. ^{1}H NMR (500 MHz, CD$_2$Cl$_2$) δ (ppm) 8.68–8.50 (m, 2H), 7.84–8.76 (m, 6H), 7.60–7.46 (m, 8H), 7.12 (t, J = 7.7 2H), 7.01 (dt, J = 7.7, 1.8 Hz, 4H), 6.94 (s, 4H), 6.79 (t, J = 8.9 Hz, 4H), 6.63 (dt, J = 8.9, 1.2 Hz, 2H), 6.22 (dd, J = 6.4, 1.7 Hz, 1H), 5.59 (m, 2H), 2.30 (s, 6H), 1.94 (s, 6H), 1.87 (s, 6H), 1.53 (s, 2H). ^{13}C NMR (126 MHz, CD$_2$Cl$_2$) δ (ppm): 164.16, 153.02, 152.92, 148.84, 148.30, 138.57, 134.60, 134.38, 134.15, 132.47, 132.14, 130.63, 129.73, 128.66, 128.58, 128.42, 127.89, 127.98, 125.50, 125.33, 124.46, 113.84, 113.70, 100.00, 20.75, 20.04. ^{19}F NMR (162 MHz, CD$_2$Cl$_2$) δ (ppm): −72.8, −74.4, −106.4, −108.0 ^{31}P NMR (162 MHz, CD$_2$Cl$_2$) δ (ppm): −20.2, −145.23 (hept). FT NSI$^+$ MS: [M − PF$_6$]$^+$ Calculated (C$_{66}$H$_{54}$F$_4$IrN$_2$P$_2$): 1205.3328; Found: 1205.3302.

Iridium(III)bis[2-(2,4-difluorophenyl)pyridinato]-bis[1,2-bis-(diphenylphosphino)ethene] hexafluorophosphate, [Ir(dFppy)$_2$-(dppe)](PF$_6$) (3c). Yield: 90%. R_f: 0.20 (DCM + 5% MeOH). Mp: 346–348 °C. ^{1}H NMR (500 MHz, CD$_2$Cl$_2$) δ (ppm): 8.52–8.35 (m, 2H), 8.87 (dd, J = 7.9, 2.8 Hz, 2H), 7.74 (t, J = 8.5 Hz, 4H), 7.57 (t, J = 8.0 Hz, 2H), 7.55–7.42 (m, 6H), 7.11 (t, J = 7.4 Hz,

2H), 6.92 (t, J = 7.7, 4H), 6.63 (dd, J = 9.2, 2.4 Hz, 2H), 6.56 (t, J = 9.5 Hz, 4H), 6.35 (t, J = 6.3 Hz, 2H), 5.79 (m, 2H), 2.12 (s, 2H). ^{13}C NMR (126 MHz, CD$_2$Cl$_2$) δ (ppm): 164.05, 160.64, 153.16, 148.59, 148.32, 148.05, 138.70, 132.62, 132.56, 132.19, 130.17, 129.92, 129.86, 129.50, 129.46, 129.43, 128.68, 128.62, 128.50, 128.14, 127.44, 126.78, 126.39, 124.14, 123.97, 123.35, 113.93, 113.78, 100.19, 99.98, 99.76. ^{19}F NMR (162 MHz, CD$_2$Cl$_2$) δ (ppm): −72.8, −74.4, −106.3, −108.0. ^{31}P NMR (162 MHz, CD$_2$Cl$_2$) δ (ppm): −21.56, −145.23 (hept). FT NSI$^+$ MS: [M − PF$_6$]$^+$ Calculated (C$_{48}$H$_{34}$F$_4$IrN$_2$P$_2$): 969.1763; Found: 969.1733.

Iridium(III)bis[2-phenylpyridinato]-bis[1,2-bis(diphenylphos-phino)ethane] hexafluorophosphate, [Ir(ppy)$_2$(sdppe)](PF$_6$) (1d). Yield: 82%. R_f: 0.23 (DCM + 3% MeOH). Mp: 156–164 °C. ^{1}H NMR (500 MHz, CD$_2$Cl$_2$) δ (ppm): 7.63 (q, J = 8.6 Hz, 6H), 9.03 (t, J = 7.9 Hz, 4H), 7.37 (t, J = 8.4 Hz, 2H), 7.30 (t, J = 8.2 Hz, 2H), 7.23 (dd, J = 6.2 Hz, 4H), 6.98 (t, J = 7.3 Hz, 2H), 6.89 (q, J = 14.6 Hz, 4H), 6.81 (t, J = 6.0 Hz, 4H), 6.58 (t, J = 8.92 Hz, 4H), 6.25 (m, 4H), 3.84 (dd, J = 10.0 Hz, 2H), 2.74 (d, J = 6.08 Hz, 2H). ^{13}C NMR (126 MHz, CD$_2$Cl$_2$) δ (ppm): 151.51, 141.23, 135.31, 131, 130.21, 129.29, 128.30, 127.20, 127.16, 126.62, 126.58, 122.83, 121.47, 112.04, 118.11, 66.42, 20.96. ^{31}P NMR (162 MHz, CD$_2$Cl$_2$) δ (ppm): −10.79, −145.23 (hept). HR NSI$^+$ MS: [M − PF$_6$]$^+$ Calculated: (C$_{48}$H$_{40}$IrN$_2$P$_2$): 899.2296; Found: 899.2297.

Iridium(III)bis[2-phenylpyridinato]-4,5-bis(diphenylphosphino)-9-isopropylxanthene hexafluorophosphate, [Ir(ppy)$_2$(isopropxant-phos)](PF$_6$) (1f). Yield: 55%. R_f: 0.25 (DCM + 3% MeOH). Mp: 285–292 °C (degraded). ^{1}H NMR (500 MHz, CD$_2$Cl$_2$) δ (ppm): 8.43 (s, 2H), 7.87 (t, J = 7.2 Hz, 4H), 7.60 (d, J = 7.6 Hz, 2H), 7.17 (t, J = 7.6 Hz, 2H), 7.09 (m, 6H), 6.87 (t, J = 6,6 Hz, 4H), 6.79 (t, J = 9.4 Hz, 4H), 6.64 (t, J = 7.4 Hz, 4H), 6.38 (t, J = 8.3 Hz, 4H), 6.30 (t, J = 7.6 Hz, 2H), 2.14 (s, 6H). ^{13}C NMR (126 MHz, CD$_2$Cl$_2$) δ (ppm): 168.11, 141.86, 138.80, 135.41, 134.48, 132.44, 132.37, 130.96, 129.67, 128.55, 128.49, 128.15, 128.08, 124.24, 123.65, 122.99, 121.33, 120.34, 68.33, 30.97, 23.66, 22.86. ^{31}P NMR (162 MHz, CD$_2$Cl$_2$) δ (ppm): −19.09, −145.23 (hept). HR NSI$^+$ MS: [M − PF$_6$]$^+$ Calculated (C$_{62}$H$_{48}$IrN$_2$OP$_2$): 1091.2871; Found: 1091.2863.

Iridium(III)bis[2-phenylpyridinato]-4,6-bis(diphenylphosphino)-phenoxazine hexafluorophosphate, [Ir(ppy)$_2$(nixantphos)](PF$_6$) (1e). Yield: 62%. R_f: 0.24 (DCM + 3% MeOH). Mp: 297–305 °C (degraded). ^{1}H NMR (500 MHz, CD$_2$Cl$_2$) δ (ppm): 8.92 (d, J = 5.2 Hz, 2H), 7.90 (m, 4H), 7.30 (t, J = 8.0 Hz, 4H), 7.17 (t, J = 7.8 Hz, 2H), 7.07 (t, J = 8.0 Hz, 4H), 6.88 (m, 14H), 6.65 (t, J = 8.1 Hz, 2H), 6.46 (t, J = 7.9 Hz, 4H), 6.29 (t, J = 8.2 Hz, 4H), 5.27 (d, J = 8.0 Hz, 2H). ^{13}C NMR (126 MHz, CD$_2$Cl$_2$) δ (ppm): 154.82, 138.50, 134.42, 134.38, 132.30, 132.27, 130.85, 130.00, 129.68, 129.39, 128.46, 128.06, 128.03, 127.99, 125.48, 124.52, 124.10, 123.69, 122.79, 120.33, 116.81. ^{31}P NMR (162 MHz, CD$_2$Cl$_2$) δ (ppm): −21.51, −145.23 (hept). HR NSI$^+$ MS: [M − PF$_6$]$^+$ Calculated (C$_{58}$H$_{43}$IrN$_3$OP$_2$): 1052.25; Found: 1052.2487.

X-ray crystallography

Single crystals were grown by vapour diffusion of ether into concentrated CH$_2$Cl$_2$ solution (2a, 3c, 4b and 4c), and by slow

230 | Inorg. Chem. Front., 2016, 3, 218–235

This journal is © the Partner Organisations 2016

evaporation of mixed solutions of CH_2Cl_2/hexane (**1a**, **1b**, **1c** and **1e**) or CH_2Cl_2/heptane (**4a**). Data were collected at either 173 K (**1a**, **1b**, **1c**, **1e**, **3c**, **4b** and **4c**) or 93 K (**4a**) on a Rigaku FR-X Ultrahigh brilliance Microfocus RA generator/confocal optics and Rigaku XtaLAB P200 system, with Mo Kα radiation (λ = 0.71075 Å), or (**2a**) at 173 K on a Rigaku MM-007HF High brilliance RA generator/confocal optics and Rigaku XtaLAB P100 system, with Cu Kα radiation (λ = 1.54187 Å). Intensity data were collected using ω steps (or ω and φ steps for **2a**) accumulating area detector images spanning at least a hemisphere of reciprocal space. All data were corrected for Lorentz polarization effects, and a multiscan absorption correction was applied by using CrystalClear.[38] Structures were solved by Patterson methods (PATTY)[39] and refined by full-matrix least-squares against F^2 (SHELXL-2013).[40] Non-hydrogen atoms were refined anisotropically, and hydrogen atoms were refined using a riding model, except for the NH hydrogen in **1e**, which was located from the difference Fourier map and refined subject to a distance restraint. All calculations were performed using the CrystalStructure interface.[41]

Photophysical measurements

All samples were prepared in HPLC grade acetonitrile with varying concentrations in the order of μM. Absorption spectra were recorded at room temperature using a Shimadzu UV-1800 double beam spectrophotometer. Molar absorptivity determination was verified by linear least-squares fit of values obtained from at least four independent solutions at varying concentrations with absorbance ranging from 6.05×10^{-5} to 2.07×10^{-5} M.

The sample solutions for the emission spectra were prepared in HPLC grade MeCN and degassed *via* three freeze–pump–thaw cycles using an in-house designed quartz cuvette. Steady state emission and excitation spectra and time-resolved emission spectra were recorded at 298 K using an Edinburgh Instruments F980. All samples for steady state measurements were excited at 360 nm while samples for time-resolved measurements were excited at 378 nm using a PDL 800-D pulsed diode laser. Emission quantum yields were determined using the optically dilute method.[32] A stock solution with absorbance of *ca.* 0.5 was prepared and then four dilutions were prepared with dilution factors between 2 and 20 to obtain solutions with absorbances of *ca.* 0.095, 0.065, 0.05 and 0.018, respectively. The Beer–Lambert law was found to be linear at the concentrations of the solutions. The emission spectra were then measured after the solutions were rigorously degassed *via* three freeze–pump–thaw cycles prior to spectrum acquisition. For each sample, linearity between absorption and emission intensity was verified through linear regression analysis and additional measurements were acquired until the Pearson regression factor (R^2) for the linear fit of the data set surpassed 0.9. Individual relative quantum yield values were calculated for each solution and the values reported represent the slope value. The equation $\Phi_s = \Phi_r(A_r/A_s)(I_s/I_r)(n_s/n_r)^2$ was used to calculate the relative quantum yield of each of the sample, where Φ_r is the absolute quantum yield of the reference, n is the

refractive index of the solvent, A is the absorbance at the excitation wavelength, and I is the integrated area under the corrected emission curve. The subscripts s and r refer to the sample and reference, respectively. A solution of quinine sulfate in 0.5 M H_2SO_4 (Φ_r = 54.6%) was used as the external reference.[29,42]

Electrochemistry measurements

Cyclic voltammetry (CV) measurements were performed on an Electrochemical Analyzer potentiostat model 600D from CH Instruments. Solutions for cyclic voltammetry were prepared in MeCN and degassed with MeCN-saturated nitrogen by bubbling for about 10 min prior to scanning. Tetra(*n*-butyl)ammoniumhexafluorophosphate (TBAPF$_6$; *ca.* 0.1 M in MeCN) was used as the supporting electrolyte. An Ag/Ag$^+$ electrode (silver wire in a solution of 0.1 M KCl in H_2O) was used as the pseudoreference electrode; a Pt electrode was used for the working electrode and a Pt electrode was used as the counter electrode. The redox potentials are reported relative to a saturated calomel electrode (SCE) electrode with a ferrocene/ferrocenium (Fc/Fc$^+$) redox couple as an internal reference (0.38 V *vs.* SCE).[33]

Electroluminescent devices

All commercial materials were used as received: aqueous dispersion of poly(3,4-ethylenedioxythiophene):poly(styrenesulfonate) (PEDOT:PSS, CLEVIOS™ P VP Al 4083; Heraeus); ionic liquid (IL) 1-butyl-3-methyl-imidazolium tetrafluoroborate [Bmim][PF$_6$] (Aldrich) and SPPO13 (Luminescence Technology Corp.). NS25 was synthetized according to the previously reported procedure.[36] The LEEC devices were made as follows. Indium tin oxide ITO-coated glass plates were patterned by conventional photolithography (Naranjo Substrates). The substrates were cleaned ultrasonically in water-soap, water and 2-propanol baths. After drying, the substrates were placed in a UV-ozone cleaner (Jelight 42–220) for 20 min. An 80 nm layer of PEDOT:PSS was spin-coated on the ITO-glass substrate. To prepare the emitting layer, the devices were spin-coated at 1000 rpm for 30 s from a solution containing either the ionic transition metal complex (iTMC) and the IL at a 4 : 1 molar ratio (iTMC : IL) or a 1 : 1 mass ratio mixture of NMS25 : SPPO13 (with 10 wt% of **4c**). After deposition of the emitting layer, the devices were transferred into an inert atmosphere glovebox, where the aluminium electrode was thermally evaporated using a shadow mask. The size of the LEEC was 6.5 mm^2.

The thickness of the films was determined with an Ambios XP-1 profilometer. Time dependence of luminance and voltage was measured by applying pulsed current and by monitoring the voltage and the luminance simultaneously by a True Colour Sensor MAZeT (MTCSICT Sensor) using a Lifetime Test System designed by BoTEST (Botest OLT OLED Lifetime-Test System). Electroluminescence spectra were recorded with an Avantes fiber-optics photo-spectrometer.

For OLED devices, ITO-coated soda lime glass substrates were cleaned by ultrasound in acetone and 2-propanol, fol-

lowed by an oxygen plasma treatment. A 40 nm thick poly(3,4-ethylenedioxythiophene):poly(styrenesulfonate) (PEDOT:PSS) was spin-coated on the ITO and baked on a hot plate at 120 °C for 10 min. A hole-transport layer of 35 nm-thick poly(N-vinyl-carbazole) (PVK) was spin-coated on the PEDOT:PSS layer and baked at 80 °C for 2 hours in a nitrogen glove box. An emissive layer of complexes blended with 1,3-bis(N-carbazolyl)benzene (mCP) and 4-diphenylphosphoryl dibenzofuran (o-DBFPPO) were spin-coated on top of the PVK layer. An electron-transport layer of 60 nm-thick bis-4,6-(3,5-di-3-pyridylphenyl)-2-methyl-pyrimidine (B3PyMPM) was deposited through a shadow mask. A cathode of Ca/Al (20 nm/200 nm) was then deposited on the B3PyMPM layer in the same vacuum system. After the evaporation, the devices were encapsulated with optical curing adhesive (Norland NOA68) and glass coverslips in the glove box. The device has an active area of 2×1.5 mm^2. The current–voltage-light output characteristics were measured using a Keithley source measure unit with a calibrated silicon photodiode. The EL spectra were measured using a charge coupled device spectrograph.

Acknowledgements

References

1 H. Sasabe and J. Kido, Development of high performance OLEDs for general lighting, *J. Mater. Chem. C*, 2013, **1**, 1699.

2 (a) F. Kessler, Y. Watanabe, H. Sasabe, H. Katagiri, M. K. Nazeeruddin, M. Grätzel and J. Kido, High-performance pure blue phosphorescent OLED using a novel bis-heteroleptic iridium(iii) complex with fluorinated bipyridyl ligands, *J. Mater. Chem. C*, 2013, **1**, 1070; (b) S. Evariste, M. Sandroni, T. W. Rees, C. Roldan-Carmona, L. Gil-Escrig, H. J. Bolink, E. Baranoff and E. Zysman-Colman, Fluorine-free blue-green emitters for light-emitting electrochemical cells, *J. Mater. Chem. C*, 2014, **2**, 5793; (c) J. Zhuang, W. Li, W. Su, Y. Liu, Q. Shen, L. Liao and M. Zhou, Highly efficient phosphorescent organic light-emitting diodes using a homoleptic iridium(III) complex as a sky-blue dopant, *Org. Electron.*, 2013, **14**, 2596.

3 (a) For a perspective on the correlation between structure and quantum yields in neutral iridium(III) complexes see: Y. You and S. Y. Park, Phosphorescent iridium(iii) com-

plexes: toward high phosphorescence quantum efficiency through ligand control, *Dalton Trans.*, 2009, 1267; (b) M. S. Lowry and S. Bernhard, Synthetically Tailored Excited States: Phosphorescent, Cyclometalated Iridium (III) Complexes and Their Applications, *Chem. – Eur. J.*, 2006, **12**, 7970; (c) S. Lamansky, P. Djurovich, D. Murphy, F. Abdel-Razzaq, H.-E. Lee, C. Adachi, P. E. Burrows, S. R. Forrest and M. E. Thompson, Highly Phosphorescent Bis-Cyclometalated Iridium Complexes: Synthesis, Photophysical Characterization, and Use in Organic Light Emitting Diodes, *J. Am. Chem. Soc.*, 2001, **123**, 4304; (d) S. Lamansky, P. Djurovich, D. Murphy, F. Abdel-Razzaq, R. Kwong, I. Tsyba, M. Bortz, B. Mui, R. Bau and M. E. Thompson, Synthesis and Characterization of Phosphorescent Cyclometalated Iridium Complexes, *Inorg. Chem.*, 2001, **40**, 1704.

4 (a) C. Ulbricht, B. Beyer, C. Friebe, A. Winter and U. S. Schubert, Recent Developments in the Application of Phosphorescent Iridium(III) Complex Systems, *Adv. Mater.*, 2009, **21**, 4418; (b) L. Wang, N. Wang, Y. Zhang, H. He and J. Zhang, Color tuning from red to green of bis-cyclometalated iridium(III) emitters based on benzoimidazole ligands in OLEDs: A DFT and TD-DFT investigation, *Synth. Met.*, 2014, **194**, 160.

5 (a) J.-S. Lu, H.-F. Chen, J.-C. Kuo, R. Sun, C.-Y. Cheng, Y.-S. Yeh, H.-C. Su and K.-T. Wong, Efficient solid-state white light-emitting electrochemical cells employing embedded red color conversion layers, *J. Mater. Chem. C*, 2015, **3**, 2802; (b) J. Qiao, L. Duan, L. Tang, L. He, L. Wang and Y. Qiu, High-efficiency orange to near-infrared emissions from bis-cyclometalated iridium complexes with phenyl-benzoquinoline isomers as ligands, *J. Mater. Chem.*, 2009, **19**, 6573.

6 (a) A. F. Henwood, S. Evariste, A. M. Z. Slawin and E. Zysman-Colman, Rigid biimidazole ancillary ligands as an avenue to bright deep blue cationic iridium(iii) complexes, *Faraday Discuss.*, 2014, **174**, 165; (b) S.-J. Yun, H.-J. Seo, M. Song, S.-H. Jin and Y. I. Kim, Blue Emitting Cationic Iridium Complexes Containing Two Substituted 2-Phenylpyridine and One 2,2′-Biimidazole for Solution-Processed Organic Light-Emitting Diodes (OLEDs), *Bull. Korean Chem. Soc.*, 2012, **33**, 3645.

7 S. B. Meier, W. Sarfert, J. M. Junquera-Hernández, M. Delgado, D. Tordera, E. Ortí, H. J. Bolink, F. Kessler, R. Scopelliti, M. Grätzel, M. K. Nazeeruddin and E. Baranoff, A deep-blue emitting charged bis-cyclometalated iridium(iii) complex for light-emitting electrochemical cells, *J. Mater. Chem. C*, 2013, **1**, 58.

8 (a) E. Orselli, G. S. Kottas, A. E. Konradsson, P. Coppo, R. Fröhlich, L. De Cola, A. van Dijken, M. Büchel and H. Börner, Blue-Emitting Iridium Complexes with Substituted 1,2,4-Triazole Ligands, Äâ Synthesis, Photophysics, and Devices, *Inorg. Chem.*, 2007, **46**, 11082; (b) C.-H. Yang, Y.-M. Cheng, Y. Chi, C.-J. Hsu, F.-C. Fang, K.-T. Wong, P.-T. Chou, C.-H. Chang, M.-H. Tsai and C.-C. Wu, Blue-Emitting Heteroleptic Iridium(III) Complexes Suitable for

232 | *Inorg. Chem. Front.*, 2016, **3**, 218–235

This journal is © the Partner Organisations 2016

High-Efficiency Phosphorescent OLEDs, *Angew. Chem., Int. Ed.*, 2007, **46**, 2418; (*c*) J. M. Fernandez-Hernandez, S. Ladouceur, Y. Shen, A. Iordache, X. Wang, L. Donato, S. Gallagher-Duval, M. de Anda Villa, J. D. Slinker, L. De Cola and E. Zysman-Colman, Blue light emitting electrochemical cells incorporating triazole-based luminophores, *J. Mater. Chem. C*, 2013, **1**, 7440.

9 L. He, L. Duan, J. Qiao, R. Wang, P. Wei, L. Wang and Y. Qiu, Blue-Emitting Cationic Iridium Complexes with 2-(1H-Pyrazol-1-yl)pyridine as the Ancillary Ligand for Efficient Light-Emitting Electrochemical Cells, *Adv. Funct. Mater.*, 2008, **18**, 2123.

10 T. Hu, L. He, L. Duan and Y. Qiu, Solid-state light-emitting electrochemical cells based on ionic iridium(iii) complexes, *J. Mater. Chem.*, 2012, **22**, 4206.

11 S. Ladouceur and E. Zysman-Colman, A Comprehensive Survey of Cationic Iridium(III) Complexes Bearing Non-traditional Ligand Chelation Motifs, *Eur. J. Inorg. Chem.*, 2013, **2013**, 2985.

12 J. A. Gillespie, E. Zuidema, P. W. N. M. van Leeuwen and P. C. J. Kamer, in *Phosphorus(III) Ligands in Homogeneous Catalysis: Design and Synthesis*, John Wiley & Sons, Ltd, 2012, p. 1.

13 (*a*) P. Alam, P. Das, C. Climent, M. Karanam, D. Casanova, A. R. Choudhury, P. Alemany, N. R. Jana and I. R. Laskar, Facile tuning of the aggregation-induced emission wavelength in a common framework of a cyclometalated iridium(iii) complex: micellar encapsulated probe in cellular imaging, *J. Mater. Chem. C*, 2014, **2**, 5615; (*b*) C. S. Chin, M.-S. Eum, S. y. Kim, C. Kim and S. K. Kang, New Type of Photoluminescent Iridium Complex: Novel Synthetic Route for Cationictrans-Bis(2-phenylpyridinato)iridium(III) Complex, *Eur. J. Inorg. Chem.*, 2006, **2006**, 4979; (*c*) Y. Koga, N. Yoshida and K. Matsubara, PL and EL behavior of near-red luminescent metallopolymer easily prepared from phosphine-containing copolymer and chloro{bis(1-phenyl-isoquinolinato-N,C2')}iridium(III), and its monomeric analog, *J. Polym. Sci., Part A: Polym. Chem.*, 2009, **47**, 4366; (*d*) X. Shen, H. Yang, X.-H. Hu, Y. Xu, F.-L. Wang, S. Chen and D.-R. Zhu, Synthesis, crystal structure and photophysical properties of a series of new neutral iridium(III) complexes with 2-phenylpyridine, *Inorg. Chem. Commun.*, 2009, **12**, 785; (*e*) P. Alam, G. Kaur, C. Climent, S. Pasha, D. Casanova, P. Alemany, A. Roy Choudhury and I. R. Laskar, New 'aggregation induced emission (AIE)' active cyclometalated iridium(iii) based phosphorescent sensors: high sensitivity for mercury(ii) ions, *Dalton Trans.*, 2014, **43**, 16431; (*f*) P. Alam, M. Karanam, D. Bandyopadhyay, A. R. Choudhury and I. R. Laskar, Aggregation-Induced Emission Activity in Iridium(III) Diimine Complexes: Investigations of Their Vapochromic Properties, *Eur. J. Inorg. Chem.*, 2014, **2014**, 3710.

14 Y.-Y. Lyu, Y. Byun, O. Kwon, E. Han, W. S. Jeon, R. R. Das and K. Char, Substituent Effect on the Luminescent Properties of a Series of Deep Blue Emitting Mixed Ligand Ir(III) Complexes, *J. Phys. Chem. B*, 2006, **110**, 10303.

15 C. H. Lin, Y. Y. Chang, J. Y. Hung, C. Y. Lin, Y. Chi, M. W. Chung, C. L. Lin, P. T. Chou, G. H. Lee, C. H. Chang and W. C. Lin, Iridium(III) complexes of a dicyclometalated phosphite tripod ligand: strategy to achieve blue phosphorescence without fluorine substituents and fabrication of OLEDs, *Angew. Chem., Int. Ed.*, 2011, **50**, 3182.

16 (*a*) Y. C. Chiu, C. H. Lin, J. Y. Hung, Y. Chi, Y. M. Cheng, K. W. Wang, M. W. Chung, G. H. Lee and P. T. Chou, Authentic-blue phosphorescent iridium(III) complexes bearing both hydride and benzyl diphenylphosphine; control of the emission efficiency by ligand coordination geometry, *Inorg. Chem.*, 2009, **48**, 8164; (*b*) C. H. Lin, Y. Chi, M. W. Chung, Y. J. Chen, K. W. Wang, G. H. Lee, P. T. Chou, W. Y. Hung and H. C. Chiu, Heteroleptic Ir(III) complexes containing both azolate chromophoric chelate and diphenylphosphinoaryl cyclometalates; reactivities, electronic properties and applications, *Dalton Trans.*, 2011, **40**, 1132; (*c*) Y.-C. Chiu, J.-Y. Hung, Y. Chi, C.-C. Chen, C.-H. Chang, C.-C. Wu, Y.-M. Cheng, Y.-C. Yu, G.-H. Lee and P.-T. Chou, En Route to High External Quantum Efficiency (~12%), Organic True-Blue-Light-Emitting Diodes Employing Novel Design of Iridium (III) Phosphors, *Adv. Mater.*, 2009, **21**, 2221; (*d*) J.-Y. Hung, C.-H. Lin, Y. Chi, M.-W. Chung, Y.-J. Chen, G.-H. Lee, P.-T. Chou, C.-C. Chen and C.-C. Wu, Phosphorescent Ir(iii) complexes bearing double benzyldiphenylphosphine cyclometalates; strategic synthesis, fundamental and integration for white OLED fabrication, *J. Mater. Chem.*, 2010, **20**, 7682.

17 (*a*) B.-S. Du, C.-H. Lin, Y. Chi, J.-Y. Hung, M.-W. Chung, T.-Y. Lin, G.-H. Lee, K.-T. Wong, P.-T. Chou, W.-Y. Hung and H.-C. Chiu, Diphenyl(1-naphthyl)phosphine Ancillary for Assembling of Red and Orange-Emitting Ir(III) Based Phosphors; Strategic Synthesis, Photophysics, and Organic Light-Emitting Diode Fabrication, *Inorg. Chem.*, 2010, **49**, 8713; (*b*) X. Shang, D. Han, S. Guan, X. Wang and G. Zhang, Theoretical investigation on the electronic structures and phosphorescent properties of a series of Ir(III) complexes with the diphenyl(1-naphthyl)phosphine ancillary ligand, *Chem. Phys. Lett.*, 2014, **614**, 110; (*c*) F. Zhang, D. Ma, L. Duan, J. Qiao, G. Dong, L. Wang and Y. Qiu, Synthesis, characterization, and photophysical and electroluminescent properties of blue-emitting cationic iridium(III) complexes bearing nonconjugated ligands, *Inorg. Chem.*, 2014, **53**, 6596.

18 A.-F. Ma, H.-J. Seo, S.-H. Jin, U.-C. Yoon, M.-H. Hyun, S.-K. Kang and Y.-I. Kim, Novel Cationic 2-Phenylpyridine-based Iridium(III) Complexes Bearing an Ancillary Phosphine Ligand: Synthesis, Photophysics and Crystal Structure, *Bull. Korean Chem. Soc.*, 2009, **30**, 2754.

19 (*a*) S.-X. Luo, L. Wei, X.-H. Zhang, M. H. Lim, K. X. V. Lin, M. H. V. Yeo, W.-H. Zhang, Z.-P. Liu, D. J. Young and T. S. A. Hor, Enhanced Emission and Analyte Sensing by Cinchonine Iridium(III) Cyclometalated Complexes Bearing Bent Diphosphine Chelators, *Organometallics*, 2013, **32**, 2908; (*b*) M. S. Lowry, W. R. Hudson, R. A. Pascal Jr. and S. Bernhard, Accelerated Luminophore Discovery

This journal is © the Partner Organisations 2016

Inorg. Chem. Front., 2016, **3**, 218–235 | 233

through Combinatorial Synthesis, *J. Am. Chem. Soc.*, 2004, **126**, 14129; (*c*) Y. Jian, S. Peng, X. Li, X. Wen, J. He, L. Jiang and Y. Dang, Novel solid state emitting iridium complexes with reduced phosphorescence-self-quenching triggered by steric blocking phosphine ligands, *Inorg. Chim. Acta*, 2011, **368**, 37; (*d*) E. C. Constable, C. E. Housecroft, E. Schönhofer, J. Schönle and J. A. Zampese, Softening the donor set for light-emitting electrochemical cells: [Ir(ppy)2(N^N)]+, [Ir(ppy)2(P^P)]+ and [Ir(ppy)2(P^S)]+ salts, *Polyhedron*, 2012, **35**, 154.

20 (*a*) L. Donato, P. Abel and E. Zysman-Colman, Cationic iridium(iii) complexes bearing a bis(triazole) ancillary ligand, *Dalton Trans.*, 2013, **42**, 8402; (*b*) S. Ladouceur, D. Fortin and E. Zysman-Colman, Enhanced Luminescent Iridium(III) Complexes Bearing Aryltriazole Cyclometallated Ligands, *Inorg. Chem.*, 2011, **50**, 11514; (*c*) S. Ladouceur, K. N. Swanick, S. Gallagher-Duval, Z. Ding and E. Zysman-Colman, Strongly Blue Luminescent Cationic Iridium(III) Complexes with an Electron-Rich Ancillary Ligand: Evaluation of Their Optoelectronic and Electrochemiluminescence Properties, *Eur. J. Inorg. Chem.*, 2013, **2013**, 5329.

21 (*a*) J. M. Fernández-Hernández, C.-H. Yang, J. I. Beltrán, V. Lemaur, F. Polo, R. Fröhlich, J. Cornil and L. De Cola, Control of the Mutual Arrangement of Cyclometalated Ligands in Cationic Iridium(III) Complexes. Synthesis, Spectroscopy, and Electroluminescence of the Different Isomers, *J. Am. Chem. Soc.*, 2011, **133**, 10543; (*b*) M. K. Nazeeruddin, R. T. Wegh, Z. Zhou, C. Klein, Q. Wang, F. DeAngelis, S. Fantacci and M. Grätzel, Efficient Green-Blue-Light-Emitting Cationic Iridium Complex for Light-Emitting Electrochemical Cells, *Inorg. Chem.*, 2006, **45**, 9245; (*c*) F. De Angelis, S. Fantacci, N. Evans, C. Klein, S. M. Zakeeruddin, J.-E. Moser, K. Kalyanasundaram, H. J. Bolink, M. Gratzel and M. K. Nazeeruddin, Controlling Phosphorescence Color and Quantum Yields in Cationic Iridium Complexes: and A Combined Experimental and Theoretical Study, *Inorg. Chem.*, 2007, **46**, 5989; (*d*) C. Shik Chin, M.-S. Eum, S. yi Kim, C. Kim and S. Kwon Kang, Blue-Light-Emitting Complexes: Cationic (2-Phenylpyridinato)iridium(III) Complexes with Strong-Field Ancillary Ligands, *Eur. J. Inorg. Chem.*, 2007, **2007**, 372; (*e*) L. He, J. Qiao, L. Duan, G. Dong, D. Zhang, L. Wang and Y. Qiu, Toward Highly Efficient Solid-State White Light-Emitting Electrochemical Cells: Blue-Green to Red Emitting Cationic Iridium Complexes with Imidazole-Type Ancillary Ligands, *Adv. Funct. Mater.*, 2009, **19**, 2950; (*f*) M. Mydlak, C. Bizzarri, D. Hartmann, W. Sarfert, G. Schmid and L. De Cola, Positively Charged Iridium(III) Triazole Derivatives as Blue Emitters for Light-Emitting Electrochemical Cells, *Adv. Funct. Mater.*, 2010, **20**, 1812; (*g*) L. He, L. Duan, J. Qiao, D. Zhang, L. Wang and Y. Qiu, Enhanced stability of blue-green light-emitting electrochemical cells based on a cationic iridium complex with 2-(1-phenyl-1H-pyrazol-3-yl)pyridine as the ancillary ligand, *Chem. Commun.*, 2011, **47**, 6467; (*h*) M. Felici, P. Contreras-Carballada, Y. Vida,

J. M. M. Smits, R. J. M. Nolte, L. De Cola, R. M. Williams and M. C. Feiters, IrIII and RuII Complexes Containing Triazole-Pyridine Ligands: Luminescence Enhancement upon Substitution with b-Cyclodextrin, *Chem. – Eur. J.*, 2009, **15**, 13124; (*i*) L. He, L. Duan, J. Qiao, G. Dong, L. Wang and Y. Qiu, Highly Efficient Blue-Green and White Light-Emitting Electrochemical Cells Based on a Cationic Iridium Complex with a Bulky Side Group, *Chem. Mater.*, 2010, **22**, 3535; (*j*) A. B. Tamayo, S. Garon, T. Sajoto, P. I. Djurovich, I. M. Tsyba, R. Bau and M. E. Thompson, Cationic Bis-cyclometalated Iridium(III) Diimine Complexes and Their Use in Efficient Blue, Green, and Red Electroluminescent Devices, *Inorg. Chem.*, 2005, **44**, 8723; (*k*) C.-H. Yang, J. Beltran, V. Lemaur, J. Cornil, D. Hartmann, W. Sarfert, R. Fröhlich, C. Bizzarri and L. De Cola, Iridium Metal Complexes Containing N-Heterocyclic Carbene Ligands for Blue-Light-Emitting Electrochemical Cells, *Inorg. Chem.*, 2010, **49**, 9891; (*l*) H.-F. Chen, W.-Y. Hung, S.-W. Chen, T.-C. Wang, S.-W. Lin, S.-H. Chou, C.-T. Liao, H.-C. Su, H.-A. Pan, P.-T. Chou, Y.-H. Liu and K.-T. Wong, Cationic Iridium Complexes with Intramolecular π-π Interaction and Enhanced Steric Hindrance for Solid-State Light-Emitting Electrochemical Cells, *Inorg. Chem.*, 2012, **51**, 12114; (*m*) S. B. Meier, W. Sarfert, J. M. Junquera-Hernandez, M. Delgado, D. Tordera, E. Orti, H. J. Bolink, F. Kessler, R. Scopelliti, M. Gratzel, M. K. Nazeeruddin and E. Baranoff, A deep-blue emitting charged bis-cyclometallated iridium(iii) complex for light-emitting electrochemical cells, *J. Mater. Chem. C*, 2013, **1**, 58; (*n*) S. Soman, J. C. Manton, J. L. Inglis, Y. Halpin, B. Twamley, E. Otten, W. R. Browne, L. De Cola, J. G. Vos and M. T. Pryce, New synthetic pathways to the preparation of near-blue emitting heteroleptic Ir(iii)N6 coordinated compounds with microsecond lifetimes, *Chem. Commun.*, 2014, **50**, 6461; (*o*) N. Darmawan, C. H. Yang, M. Mauro, M. Raynal, S. Heun, J. Pan, H. Buchholz, P. Braunstein and L. De Cola, Efficient near-UV emitters based on cationic bis-pincer iridium(III) carbene complexes, *Inorg. Chem.*, 2013, **52**, 10756; (*p*) W.-T. Chen, Y.-J. Chen, C.-S. Wu, J.-J. Lin, W.-L. Su, S.-H. Chen and S.-P. Wang, Two new blue-phosphorescent Ir(III) cyclometalated complexes demonstrating the pushing-up effects of amino on levels of Pi-type molecular orbitals, *Inorg. Chim. Acta*, 2013, **408**, 225.

22 V. N. Kozhevnikov, Y. Zheng, M. Clough, H. A. Al-Attar, G. C. Griffiths, K. Abdullah, S. Raisys, V. Jankus, M. R. Bryce and A. P. Monkman, Cyclometalated Ir(III) Complexes for High-Efficiency Solution-Processable Blue PhOLEDs, *Chem. Mater.*, 2013, **25**, 2352.

23 C. Zhong, C. Duan, F. Huang, H. Wu and Y. Cao, Materials and Devices toward Fully Solution Processable Organic Light-Emitting Diodes, *Chem. Mater.*, 2011, **23**, 326.

24 (*a*) N. Miyaura, T. Yanagi and A. Suzuki, The Palladium-Catalyzed Cross-Coupling Reaction of Phenylboronic Acid with Haloarenes in the Presence of Bases, *Synth. Commun.*, 1981, **11**, 513; (*b*) N. Miyaura and A. Suzuki, Palladium-

234 | *Inorg. Chem. Front.*, 2016, **3**, 218–235

This journal is © the Partner Organisations 2016

Catalyzed Cross-Coupling Reactions of Organoboron Compounds, *Chem. Rev.*, 1995, **95**, 2457.

25 M. Nonoyama, Benzo[h]quinolin-10-yl-N Iridium(III) Complexes, *Bull. Chem. Soc. Jpn.*, 1974, **47**, 767.

26 F. H. Allen, The Cambridge Structural Database: a quarter of a million crystal structures and rising, *Acta Crystallogr., Sect. B: Struct. Sci.*, 2002, **58**, 380.

27 (a) S. Ladouceur, D. Fortin and E. Zysman-Colman, The role of substitution on the photophysical propertiesof 5,5′-diaryl-2,2′-bipyridine (bpy*) in [Ir(ppy)2(bpy*)]PF6 complexes: A combined experimental and theoretical study, *Inorg. Chem.*, 2010, **49**, 5625; (b) K. K.-W. Lo and J. S.-Y. Lau, Cyclometalated Iridium(III) Diimine Bis(biotin) Complexes as the First Luminescent Biotin-Based Cross-Linkers for Avidin, *Inorg. Chem.*, 2007, **46**, 700; (c) J. B. Waern, C. Desmarets, L.-M. Chamoreau, H. Amouri, A. Barbieri, C. Sabatini, B. Ventura and F. Barigelletti, Luminescent Cyclometalated RhIII, IrIII, and (DIP)2RuII Complexes with Carboxylated Bipyridyl Ligands: Synthesis, X-ray Molecular Structure, and Photophysical Properties, *Inorg. Chem.*, 2008, **47**, 3340; (d) H. J. Bolink, E. Coronado, R. n. D. Costa, N. Lardiés and E. Ortì, Near-Quantitative Internal Quantum Efficiency in a Light-Emitting Electrochemical Cell, *Inorg. Chem.*, 2008, **47**, 9149; (e) A. B. Tamayo, B. D. Alleyne, P. I. Djurovich, S. Lamansky, I. Tsyba, N. N. Ho, R. Bau and M. E. Thompson, Synthesis and Characterization of Facial and Meridional Tris-cyclometalated Iridium(III) Complexes, *J. Am. Chem. Soc.*, 2003, **125**, 7377.

28 For recent reviews see: L. Flamigni, A. Barbieri, C. Sabatini, B. Ventura and F. Barigelletti, Photochemistry and Photophysics of Coordination Compounds: Iridium, *Top. Curr. Chem.*, 2007, **281**, 143.

29 W. H. Melhuish, Quantum Efficiences Of Fluorescence Of Organic Substances: Effect Of Solvent And Concentration Of The Fluorescent Solute 1, *J. Phys. Chem.*, 1961, **65**, 229.

30 J. Wang, F.-Q. Bai, B.-H. Xia and H.-X. Zhang, Efficient Blue-Emitting Ir(III) Complexes with Phosphine Carbanion-Based Ancillary Ligand: A DFT Study, *J. Phys. Chem. A*, 2011, **115**, 11689.

31 N. M. Shavaleev, F. Monti, R. D. Costa, R. Scopelliti, H. J. Bolink, E. Ortí, G. Accorsi, N. Armaroli, E. Baranoff, M. Grätzel and M. K. Nazeeruddin, Bright Blue Phosphor-

escence from Cationic Bis-Cyclometalated Iridium(III) Isocyanide Complexes, *Inorg. Chem.*, 2012, **51**, 2263.

32 (a) H.-C. Su, F.-C. Fang, T.-Y. Hwu, H.-H. Hsieh, H.-F. Chen, G.-H. Lee, S.-M. Peng, K.-T. Wong and C.-C. Wu, Highly Efficient Orange and Green Solid-State Light-Emitting Electrochemical Cells Based on Cationic IrIII Complexes with Enhanced Steric Hindrance, *Adv. Funct. Mater.*, 2007, **17**, 1019; (b) C. Rothe, C.-J. Chiang, V. Jankus, K. Abdullah, X. Zeng, R. Jitchati, A. S. Batsanov, M. R. Bryce and A. P. Monkman, Ionic Iridium(III) Complexes with Bulky Side Groups for Use in Light Emitting Cells: Reduction of Concentration Quenching, *Adv. Funct. Mater.*, 2009, **19**, 2038.

33 V. V. Pavlishchuk and A. W. Addison, Conversion constants for redox potentials measured versus different reference electrodes in acetonitrile solutions at 25 °C, *Inorg. Chim. Acta*, 2000, **298**, 97.

34 S. van Reenen, P. Matyba, A. Dzwilewski, R. A. J. Janssen, L. Edman and M. Kemerink, Salt Concentration Effects in Planar Light-Emitting Electrochemical Cells, *Adv. Funct. Mater.*, 2011, **21**, 1795.

35 S. van Reenen, R. A. J. Janssen and M. Kemerink, Doping dynamics in light-emitting electrochemical cells, *Org. Electron.*, 2011, **12**, 1746.

36 A. Pertegás, N. M. Shavaleev, D. Tordera, E. Ortí, M. K. Nazeeruddin and H. J. Bolink, Host–guest blue light-emitting electrochemical cells, *J. Mater. Chem. C*, 2014, **2**, 1605.

37 (a) S. E. Jang, K. S. Yook and J. Y. Lee, High power efficiency in simplified two layer blue phosphorescent organic light-emitting diodes, *Org. Electron.*, 2010, **11**, 1154; (b) J. Wang, X. Xu, Y. Tian, C. Yao, R. Liu and L. Li, A novel blue fluorescent polymer for solution-processed fluorescent-phosphorescent hybrid WOLEDs, *J. Mater. Chem. C*, 2015, **3**, 2856.

38 *CrystalClear-SM Expert v. 2.1*, The Woodlands, Texas, USA, 2010–2014.

39 P. T. Beurskens, G. Beurskens, R. de Gelder, S. Garcia-Granda, R. O. Gould, R. Israel and J. M. M. Smits, *DIRDIF-99. DIRDIF-99*, University of Nijmegen, The Netherlands, 1999.

40 G. Sheldrick, Crystal structure refinement with SHELXL, *Acta Crystallogr., Sect. C: Cryst. Struct. Commun.*, 2015, **71**, 3.

41 *CrystalStructure v 4.1*, The Woodlands, Texas, USA, 2014.

42 A. M. Brouwer, Standards for photoluminescence quantum yield measurements in solution (IUPAC Technical Report)*, *Pure Appl. Chem.*, 2011, **83**, 2213.

This journal is © the Partner Organisations 2016

Inorg. Chem. Front., 2016, **3**, 218–235 | 235